# THE INFLUENCE OF THE RATE OF DEFORMATION ON THE STRENGTH OF MATERIALS IN TENSION

Thesis

by

LeVan Griffis

In Partial Fulfillment of the Requirements

for the Degree of

Doctor of Philosophy

California Institute of Technology

Pasadena, California

1941.

ACKNOWLEDGMENT

The author wishes to acknowledge his appreciation to the sponsors of the Impact Research Program who have made this investigation possible: namely, General Petroleum Corporation of California, Hughes Tool Company, International Nickel Company, Lane-Wells Company, National Advisory Committee for Aeronautics, and Union Oil Company of California.

Appreciation is extended to Dr. D. S. Clark for his inspiring directorship of the research program, and for his valuable assistance and criticism in this work; and to E. E. Simmons, Jr., for his assistance in the design and development of the high velocity testing machine, and to all the others who have aided in the furtherance of this research.

Sincere thanks are extended to Mrs. Alice Gazin for her diligence in the preparation of the typewritten manuscript, and to Donald C. Campbell for his assistance in preparing the data in their final form.

CONTENTS

## ABSTRACT

There is growing significance to the tension impact test in comparing the usefulness of materials for service conditions in which dynamic loading occurs. Many recent investigations have begun the study of the dynamic properties of materials, and have attempted to correlate their results with the existing theories of strength of materials. Few investigators have succeeded in developing their experimental procedure in impact testing to the point of determining basic tensile properties measured by the stress-strain diagram.

This thesis discusses a method of determining stress-strain relations for materials under tension impact loads at various speeds. Tension characteristics of eight different engineering alloys are discussed for rates of deformation from 10 to 190 feet per second. Comparison with results from static tests is made for these materials, and the influence of the rate of deformation is noted.

The results indicate that in general, for the materials tested, the yield and ultimate stresses under dynamic conditions are higher than for static conditions; and quantitative data are tabulated as a function of the rate of deformation. The dynamic energies absorbed in tension impact are usually larger than the static values, but they may decrease in the case of certain heat treated steels. Results do not indicate a critical velocity of embrittlement for any of the materials tested within the range of velocities reported. Use of any single type of geometrical deformation of the material as a measure of the resistance of the material to dynamic loads is not found possible.

Application of this test procedure is suggested as a basis for investigating the relative usefulness of different heat treatments and alloying of metals for service conditions involving dynamic tensile loading.

# THE INFLUENCE OF THE RATE OF DEFORMATION ON THE STRENGTH OF MATERIALS IN TENSION

## Chapter I

## Brief History of Tension Impact Testing

A. General: Significance of Various Types of Impact Tests.—Two basically important factors in determining the strength of materials seem to be the rate of deformation, and the temperature. This thesis deals with an investigation of the effect of varying the rate of deformation on the strength of materials during tension impact loading. "Impact testing" refers to a study of the behavior of materials under application of suddenly applied loads, or to a study of the effect of the rapid deformation of materials. In engineering terms, "impact testing" has in the past implied primarily the testing of notched specimens in bending, though this latter type of test is more properly referred to as a "notched bar test in bending." In general, there are three types of impact tests in common use: namely, bending impact tests, of which notched bar tests are the most common; torsion impact tests; and tension impact tests.

For bending impact, the most common machine in use is a pendulum so constructed as to permit fracture of small beams struck horizontally, at the mid-span if simply supported (Charpy type) or near the support if cantilevered (Izod type), by the center of percussion of the pendulum hammer. Beams of ductile material must be notched across the side opposite the hammer if rupture is desired. The change in the

kinetic energy of the pendulum during fracture closely approximates the energy consumed by the specimen. Other types of machines employ a rapidly rotating disc with jaws at the periphery, in the path of which a bending specimen may be introduced. In this case the energy required to rupture may be determined from the change in kinetic energy of the disc or by holding the specimen in a pendulum and measuring the change in kinetic energy of the pendulum due to the reaction of the specimen.

In torsion testing, a twist is applied suddenly to a cylindrical specimen. This is accomplished by fixing a specimen from rotating at one end, and holding it such that the other end can be engaged circumferentially by a clutch attached to a disc rotating at the desired speed. The energy required to fracture the specimen is obtained approximately by measuring the accompanying loss of kinetic energy of the rotating disc as indicated by the change of angular speed. This type of test has been developed and found useful primarily for determining impact characteristics of extremely hard materials such as tool steels. The pendulum (Izod or Charpy) tests are not so well suited for tests on these materials because of the small amount of energy required to break them. Since tool steels are normally quite brittle, the presence of a notch makes the accurate measurement of impact energy values difficult.

In tension impact tests, a load is applied either by a pendulum or a rotating disc in such a manner that a cylindrical specimen, firmly anchored at one end, is pulled apart in tension by the load applied at the other end. Though no one type of machine has been universally approved for this purpose, this type of test is receiving

increasing attention in engineering circles for several reasons. The relatively complex stress conditions existing in a specimen subjected to failure in bending are apparent. In the Charpy and Izod bending tests, these complex stress conditions are increased by the presence of a notch. Such procedure causes high concentrations of stress in the vicinity of the notch--rendering the results of such tests purely qualitative. Correlation with other physical properties of the absorbed energy values obtained from such tests has never been satisfactory; in fact, correlation with service conditions can only be made for the characteristic of notch sensitivity. For ductile materials at least, since small eccentricities of loading have little effect on the energy of rupture, tensile impact tests are more accurate than notched bar transverse tests. In attempting to study the effect of the rate of deformation on the properties of materials, it will be noted that a high torsional speed may not correspond to a very high rate of strain of the actual fibers of the material. A rate of twist of 700 revolutions per minute on a 1/2 inch diameter specimen corresponds to a strain rate at the extreme fibers of only 1.4 feet per second.

Many of the significant mechanical properties of a material are expressed by the tensile and shear properties obtained from a tension test; consequently this type of impact test should give more basic quantitative information than can be obtained from a notched bar test. In addition, if the effects of rate of deformation together with temperature variation on tensile properties are to be investigated, a tension impact should be employed. Finally, this type of test lends itself to a determination of stress-strain relations during impact

loading, from which the important physical properties of yield stress, ultimate and breaking stress, and energy absorbed, as well as reduction of area and per cent elongation, may all be determined.

B. Results of Some Earlier Investigations.--The fact that forces, under which ductile metals yield continuously, increase in general if the speed of deformation is increased, was noted by early investigators of the mechanical properties of materials. In 1909 Ludwik[1] mentioned the influence of the speed of plastic deformation, stating that the internal resistance of a metal to permanent change in shape increases with the permanent strains and also with the rate of strain. In tension experiments with tin wires, he came to the conclusion that the ultimate load increases with the log of the strain rate.[2] The same conclusion is discussed by Prandtl,[3] who, with a mechanical model of a solid body, indicates for a certain range of plastic rates of strain that the logarithmic speed law gives a general expression connecting the rate of strain with the yield force.

Several recent investigations have been made describing the plastic behavior of ductile metals under simple states of tensile or compressive stress when the velocity of plastic deformation is increased.[4] Koerber and Storp[5] found for four carbon steels that the ultimate strength from calculated dynamic tensile stress-strain curves was 1.15 to 1.42 times larger and the per cent elongation at rupture was 1.05 to 1.12 times larger than corresponding static values. Average rates of strain were of the order of 8 feet per second. Honegger[6] computed loads in tension impact tests by double differentiation of the recorded relative motion between the two heads of the test specimens. The rate of strain

during each test varied from about 12 to 5 feet per second. He found for soft aluminum and copper that the tensile strengths and elongations at rupture were about one and one quarter times the static values, while for hard copper and aluminum these values were somewhat less. Energy absorbed up to rupture was 30 to 40 per cent larger for the dynamic tests than for the static.

Weerts[7] investigated the effect of the speed of deformation on stress-strain curves of single-crystal bars of pure aluminum tested in tension, with specimens of gage length of 100 millimeters, and diameter of 3.4 millimeters. The mean rate of strain was about one foot per second. The results showed that the ultimate tensile strength was dynamically about 18 per cent higher than statically.

In all the preceding experimental work, either the pendulum or drop-weight type of machine was used. Consequently the speeds of impact were limited to very low values--less than 15 feet per second. In addition, the velocity during any one test was variable due to the fact that the energy required to rupture the specimens was usually an appreciable amount of the available kinetic energy of the hammer. By decreasing the velocity of impact this fault was greatly amplified, since the available energy varies with the square of the velocity. In addition, the dynamic stress-strain curves referred to were indirectly derived, being calculated from the curve showing the observed length of the test specimen as a function of time "t" during stretching by the falling hammer or pendulum. Knowing the mass of the falling weight, and obtaining the retardation $d^2l/dt^2$ by double differentiation of the empirical curve $l = f(t)$, the tensile loads may be found under

which the bar is stretched. This double differentiation of an empirical curve is hardly convenient or satisfactorily exact for rapid testing, however.

A rotary type of impact machine was introduced in France by Guillery[8] in which the kinetic energy of a flywheel is used for breaking notched specimens in bending. Available velocities of impact are of the order of 18 feet per second, and the energy required to rupture the specimen is obtained from the change in speed of the wheel measured by an hydraulic tachometer. Moore[9] used the elastic extension of a steel bar to measure the force on a tension test specimen rapidly loaded by a falling weight. A few high speed tension stress-strain curves were recorded by D. W. Ginns,[10] with a machine in which a large elastic spring served for loading. Forces were measured by means of a carbon substance whose electrical resistance varied with the pressure exerted on it. The rates of strain investigated were of the order of 5 feet per second.

A rotary impact machine capable of producing tension impact tests at rates up to 350 feet per second was recently described by H. C. Mann.[11] This equipment recorded impact energies up to rupture, but not stress-strain diagrams. The most outstanding result was the observation of a "transition" velocity or critical rate of tensile deformation for each material tested, above which the impact energy seemed to decrease rapidly with increasing strain rate. He also measured per cent elongation and reduction of area, and produced such data as shown in Figure 3, page 13 of this paper.

Many other investigations have been made in the field of impact testing, but most of them have to do with notched bar tests in

bending. One group of experimentors in particular, working in the laboratories of the Physico-Technical Institute in Leningrad under the supervision of N. N. Davidenkoff,[12] have made an investigation of the effect of velocity on bend tests over a velocity range from static to 350 feet per second, using a rotary disc for the higher range. Energy values only were recorded, and nominal stress-strain values during rupture were calculated and compared on the basis of simple beam formulas. These data are discussed later on page 12. As in most of the investigations mentioned above, only the values of energy, reduction of area, and per cent elongation were obtained directly.

Practically all of the results of these projects have been limited either in the range of velocities attainable, or in the possibility of direct and reliable measurement of actual stresses as well as energies, or in both respects.

## Chapter II

## Some Theoretical Considerations Concerning Tension Testing

A. Cohesive Strength and the Resistance to Plastic Deformation.— Information obtained by investigators during the past twenty years has shown qualitatively that ductility and total energy required to rupture a material depend on the relation between resistance to fracture and the resistance to plastic deformation. The normal stress required to cause failure by separation across a transverse section of a tension test bar is called the "cohesive strength" of the material. In a ductile material, this cohesive strength is sufficiently large to support the normal load; consequently the maximum shear stress induced at 45 degrees with the axis of the test bar produces plastic deformation. As the material is deformed plastically, its resistance to shear deformation increases, until it reaches a value equal to the cohesive strength, when it fails in simple tension. If the tensile stress required to produce plastic deformation is less than the resistance to fracture, plastic flow precedes fracture and a relatively larger energy is absorbed. If the resistance to plastic flow is larger than the resistance to fracture, a brittle failure occurs with a smaller absorption of energy.

Though ductility of a material is generally considered to be assurance that it will not fail without plastic deformation, service conditions may be such that the resistance to flow is higher than the resistance to cohesive failure. In this case, the failure will be brittle rather than ductile in nature and the amount of energy required to produce failure may be greatly decreased.

In a standard static tension test, fracture occurs after more or less plastic extension; hence the resistance to fracture, obtained by dividing the breaking load by the corresponding sectional area is not the cohesive strength of the original material but of metal plastically deformed. By such plastic deformation, the cohesive strength is greatly altered.

In order to obtain the cohesive strength of a given material in any specified condition of plastic deformation the following procedure is suggested by W. Kuntze in his paper entitled "Questions of Technical Cohesion."[13] Several cylindrical specimens of this same material are prepared with identical notches of different depths. Plotting the stress to cause failure against the reduction of area due to the notch, and extrapolating to zero area or 100 per cent reduced section, the stress indicated by this extrapolation is taken as the cohesive strength of the given material. This is represented in Figure 1.[13] The notching of the specimens is required to increase the resistance to deformation so that it exceeds the cohesive strength by limiting the plastic strain. This straight line does not give any true stresses except at the point of separation failure, because only there has plastic deformation ceased entirely, and consequently there are no variations in stress distribution due to notch effect.

In general, the relationship between the cohesive strength and the resistance to shear deformation depends not only on the material, but on its structural characteristics due to the degree of prior plastic deformation, the velocity of strain, temperature, combination of stresses, form and size of specimen, and presence of notches. The influence of

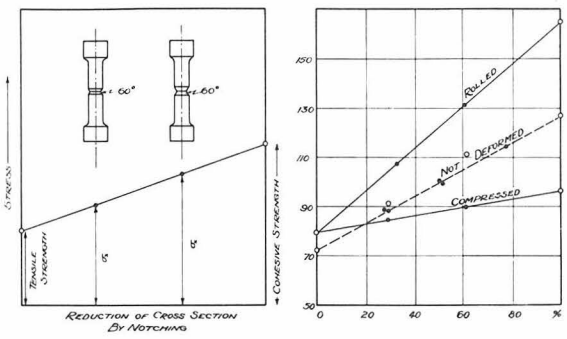


Fig. 1
Determination of Cohesive Strength

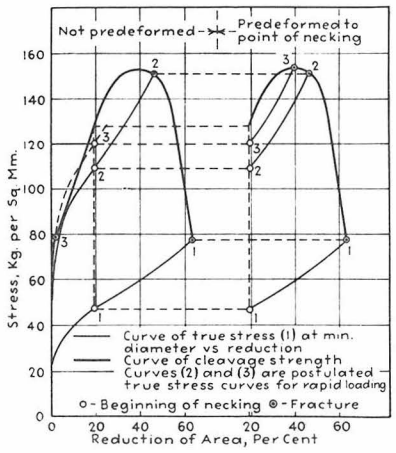


True Stress and Cleavage Strength of 0.18 Per Cent Steel vs. Deformation (Kuntze).

Fig. 2

prior plastic strain on the cohesive strength and the resistance to plastic deformation is shown in Figure 2,[13] for a 0.18 per cent carbon steel. The amount of cold working during testing is represented by abscissas in per cent reduction of area. The lower curve represents the resistance to deformation, which rises steadily; the upper curve gives the cohesive strength, which first rises then descends. The true breaking stress is that stress where the resistance to deformation equals the cohesive strength. Thus for a ductile material at room temperature, which is deformed plastically at a slow rate, the cohesive strength first increases abruptly, while the resitance to deformation rises gradually.

Investigations with notched bar impact tests have shown that up to certain limits a bar may absorb more energy as the speed of deformation is increased above static conditions. When the rate of strain reaches a certain value, the energy expended may decrease and the fracture change from a ductile to a brittle type. In other words, the resistance to deformation (true stress) has apparently increased with the rate of strain up to certain speeds. Increasing the speed of deformation, therefore, may be expected to raise the true stress curve above the static curve, as represented by the postulated curves (2) and (3) in the left half of Figure 2. For curve (2), failure occurs when the true stress equals the cohesive strength. Curve (3), for a higher velocity, shows the intersection at a much lower stress, with a very brittle fracture almost without deformation. The curves in the right half of Figure 2 show the same postulated stress-strain relations for a bar of the same material deformed before testing by reducing the area about 20 per cent. In this case a test velocity corresponding to curve (3) will not show

failure till the stress reaches a very high value at the peak of the cohesive strength curve, resulting in a ductile fracture.

B. Effect of Velocity on the Energy of Rupture.---A somewhat contrasting theoretical possibility is suggested in the results of the investigation by H. C. Mann.[11] The object of his work was to find the effect of velocity on the energy absorbed during tensile fracture of a specimen. Results of his tests indicated that for every material the energy absorbed up to fracture was constantly equal to the static value for all speeds up to a "critical velocity of embrittlement," after which the energy decreased abruptly to much lower values. Typical data from such a test are shown in Figure 3, for an S.A.E. 1035 Steel fully annealed. For this material the critical velocity is approximately 35 feet per second. Similar data are presented for rolled Silicon Bronze,[11] for which the critical velocity is reported as 90 feet per second. However, the reduction of area and per cent elongation seem to increase slightly at the critical velocity, for all materials tested. This would indicate that the dynamic stresses above the critical or transition velocity are in general smaller than the static values. In the absence of stress-strain diagrams corresponding to Mann's tests, no discussion of this situation was possible in his paper.

Investigations of bend testing performed in the Impact Laboratory of the Physico-Technical Institute in Leningrad[12] have endeavored to show that the temperature of the material is the determining factor in its behavior. The investigators have interpreted the effects of high velocity on bend testing in terms of the effect on the "critical temperature of embrittlement," or temperature below which a material

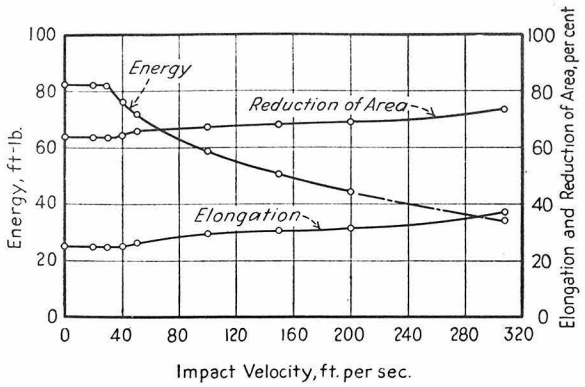


Fig. 3
Effect of Impact
Velocity on Properties
of SAE 1035 Steel, fully annealed

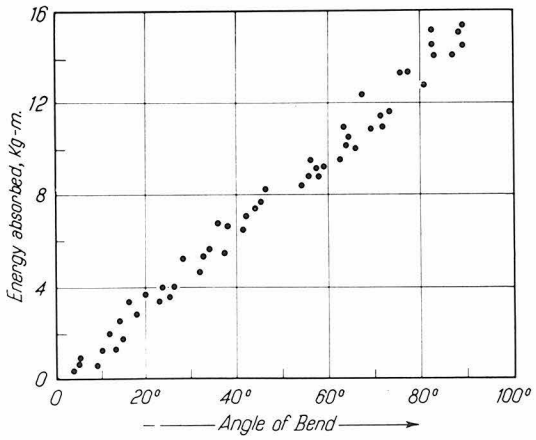


*When Unnotched Charpy Test Pieces Are Broken and Reassembled, the Angle of Bend Is Proportional to the Energy Absorbed*

Fig. 4 (Davidenkoff)

always acts in a brittle manner and above which temperature the material is always ductile. In general, an increased rate of loading has been shown to raise the critical temperature of embrittlement.

Discussion of nominal "stresses" during these bend tests is based on calculations according to simple beam theory, which are applied to all deflections of the material up to fracture. In general, a logarithmic relation has been assumed to hold between the velocity of deformation and the critical temperature of embrittlement. Direct measurement during these investigations was limited to noting the variation in angle of bend, and correlating this to the change in lateral dimension of the specimen at fracture. This dimensional property is used as a linear measure of all energy values absorbed up to fracture, basing this reasoning on an obscurely obtained experimental straight-line-relation between lateral deformation and energy absorbed (see Figure 4[12]). This is the basic premise of all the interpretations of the results of this investigation; in terms of a tension test it would be equivalent to stating that the per cent elongation, or contraction in diameter, is a direct measure of the energy absorbed up to fracture. That such a simple relation does not hold between energy and deformation is suggested later. (See page 82 of this paper.) Again, in this investigation by the Russian laboratories, absence of direct measurement of stress-strain relations or of energy values during impact tests prevented reliable verification of these results.

## Chapter III

## Object of This Investigation

The behavior of a material under conditions of tension impact loading can be shown to best advantage by means of a force-elongation diagram. To accomplish this, equipment has been developed for recording force-elongation curves during tension impact tests, with a simple method of reducing these to stress-strain relations. From such relations, the basic properties of yield, ultimate and breaking stresses, energy absorbed to rupture, per cent elongation, and per cent reduction of area can all be obtained for materials tested at rates of strain from 5 feet per second up to velocities of 200 feet per second. From such data, the effect of rate of deformation may be more rationally analyzed than heretofore possible, and comparison can be made with the results of conventional static tests.

The purpose of this thesis is threefold:

(1) The presentation of suitable testing equipment and procedure for obtaining stress-strain diagrams for materials under tension impact loading, at rates of deformation from static up to 200 feet per second.

(2) Interpreting from such testing procedure the effect of rate of deformation on the tensile characteristics of materials, that is, on the yield, ultimate, and breaking stresses, the absorbed energy, per cent elongation, and reduction of area.

(3) Discussion of such interpretations in the light of the existing theories of strength of materials, pointing out where such theories may be verified or disproved by the results of this investigation.

## Chapter IV

## Equipment and Testing Procedure

Preliminary investigation of the problem of determining stress-strain relations during tension impact tests was made with a reconstructed Tinius Olsen Izod Impact Machine, of 120 foot-pound energy capacity. This pendulum apparatus was revised so that specimens could be fractured in tension at speeds up to 11.3 feet per second, and a method was developed for recording force-time diagrams during these tests. From the inertia characteristics of the pendulum, and by a double integration of these force-time records, the corresponding displacement-time curves for the pendulum are computed, which give elongation-time relations for the specimens. Combining these with the original force-time records, stress-strain relations for the impact tests are found. Details of this procedure are described by D. S. Clark and G. Dätwyler in an article entitled "Stress-Strain Relations under Tension Impact Loading," presented before the American Society for Testing Materials in July, 1938.[14]

By simplification of this procedure, equipment was devised by the author for recording directly force-elongation diagrams at velocities up to 11.3 feet per second with the same pendulum machine. The technique used was essentially the same as described later in this thesis. Various engineering materials, including both ferrous and non-ferrous alloys, were investigated at this speed of 11.3 feet per second and the results compared with static tests. Data were of sufficient interest and the technique was found satisfactory for application to higher velocities. Consequently a rotary type tension impact machine

was designed for this purpose, capable of testing at variable speeds from 5 to 300 feet per second.

A. Construction of Apparatus.

1. Loading Equipment.—A 750 horsepower hydraulic impulse turbine with the exciter generator was obtained on loan from the Southern California Edison Company. The water-wheel buckets were removed; and the machine, with suitable electric wiring for operation either as a variable speed motor or generator, was installed in a pit 8 feet wide, 12 feet long, and 6 feet below the floor level (see Figure 5).

The disc, A in Figure 5, has a diameter of 44 inches, turns on a horizontal shaft, and together with shaft and rotor weighs approximately 2000 pounds. Suitable striking jaws, B, and counterweights, C, are connected firmly to the periphery of the wheel, as shown in Figures 5 and 6.

The normal operating speed as a water-wheel was 750 revolutions per minute, with a corresponding peripheral velocity of 150 feet per second. Reasonable overspeeding for short intervals is permissible, and provides impact velocities up to 300 feet per second. Due to the inertia of the rotating mass, and because of the relatively small amount of energy required to rupture the specimens in tension impact, the velocity of the wheel is effectively constant during fracture at any operating speed. Elongation-time measurements in support of this are discussed on page 30.

The disc can be stopped from any operating speed within 20 seconds, by operating the machine as a generator and dissipating the electric energy through a suitable resistance. As an additional safety

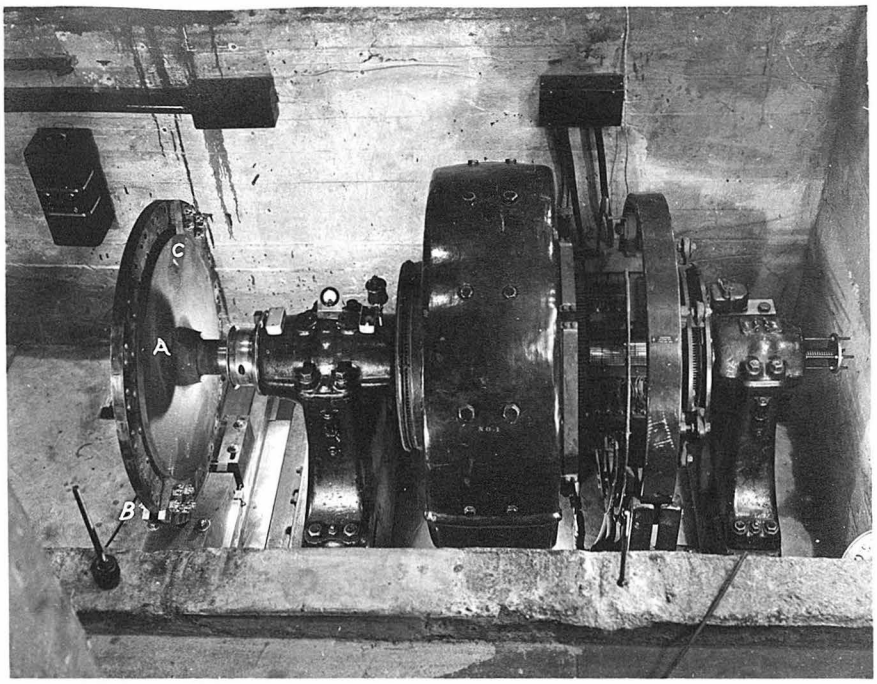


Fig. 5
Rotary Impact Tester in Pit

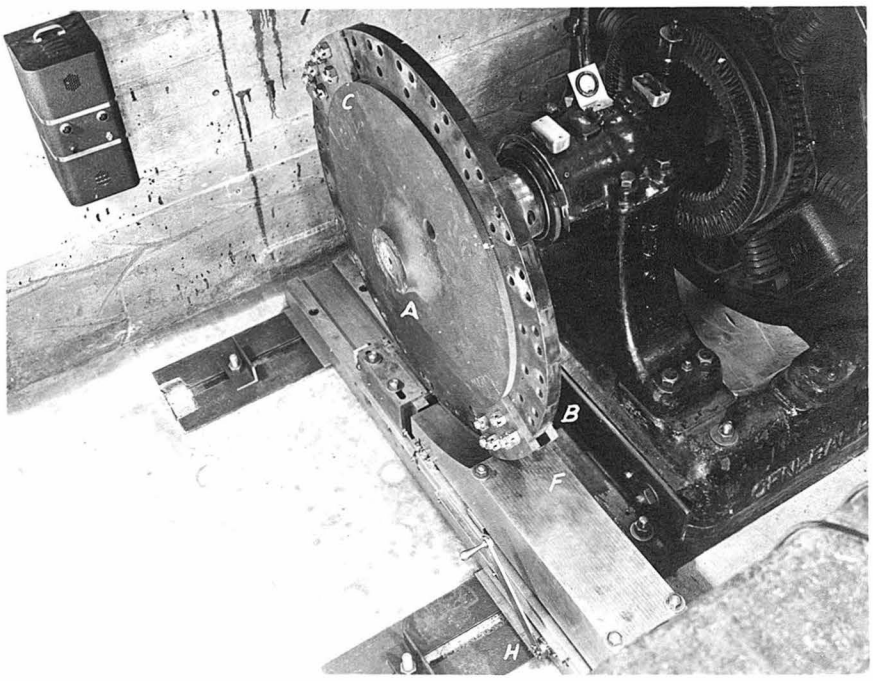


Fig. 6
Disc Showing Jaws and Counterweights

feature, the pit is covered with heavy timber bolted to the walls of the pit.

Electric control of the machine is centered above the pit at the main control panel shown at D in Figure 7.

The force-measuring unit, or dynamometer, E, into which a specimen screws, is firmly anchored in the end of a 715 pound anvil, F, machined from a 9 inch by 9 inch by 43 inch billet of steel, and shown in Figures 6 and 8. Normally this anvil is bolted rigidly to a sub-base G, Figure 8, which slides horizontally on finished ways, under the action of a gear-crank and rack shown at H in Figures 6 and 8. Thus, for the purpose of replacing specimens, the specimen holder is moved back from its usual operating position tangent to the under side of the disc, as in Figure 9.

The anvil can also be mounted on two vertical flexible fixed-end columns of clock-spring steel, 1.00 inches long and 0.015 inches thick, one under each end of the anvil, clamped as shown at I, Figure 9. This anvil is designed so that tensile forces acting on the specimen during impact pass through the center of gravity of the anvil F. Hence it may be used as an inverted pendulum. By measuring the maximum velocity imparted to this anvil during fracture of the specimen, and by computing the momentum of the anvil acting as an inverted pendulum, an independent check is possible on the amount of impulse transferred through the specimen as indicated from the force-time diagram obtained with the recording oscillograph shown at J in Figure 7 and discussed later. This provides an independent external check on the reliability of the force measurements as recorded by the testing equipment.

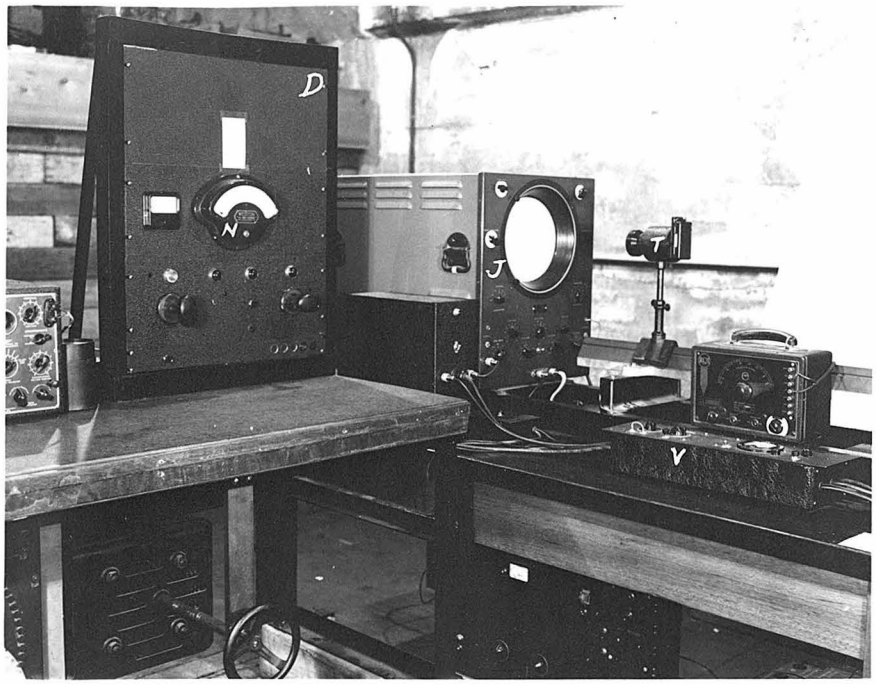


Fig. 7
Control Panel, Oscillograph, and Camera

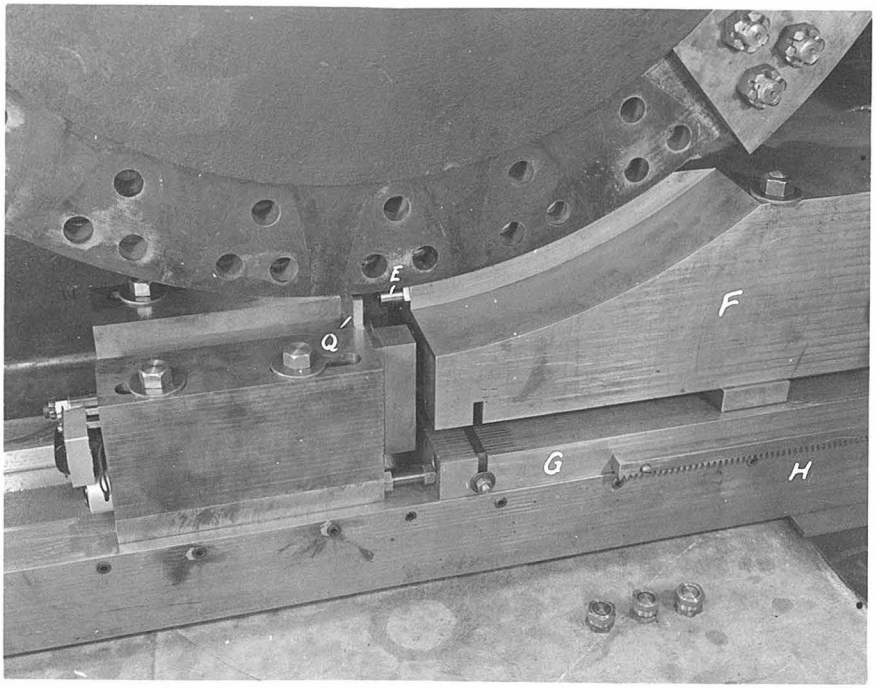


Fig. 8
Dynamometer, Anvil,
Jaws, and Yoke, before Impact

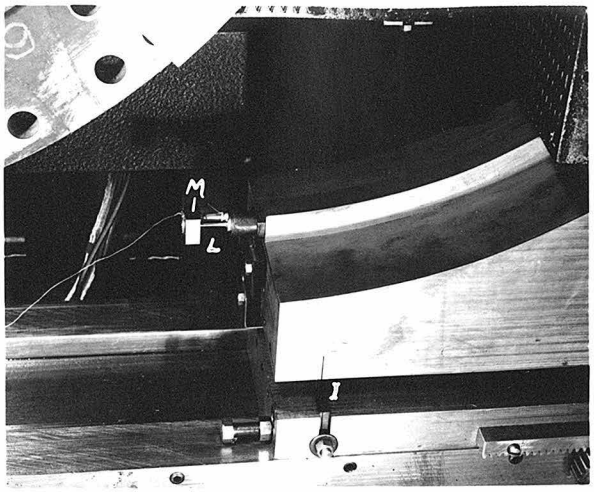


Fig. 9
Specimen, Dynamometer,
Extensometer, and Tup, Assembled

Fig. 10
Specimen just
before Impact

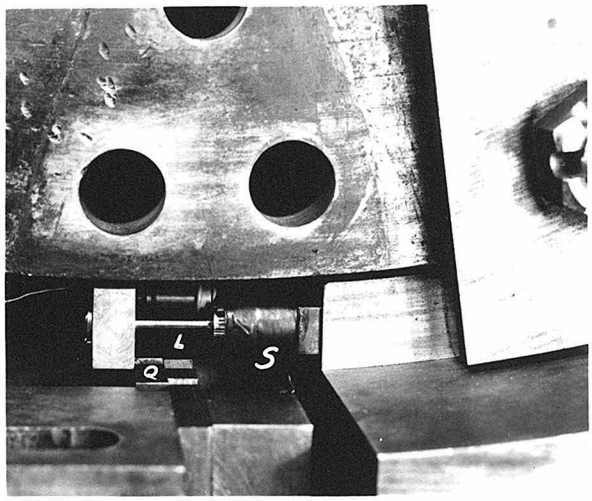


Fig. 11
Solenoid and
Trigger Mechanism

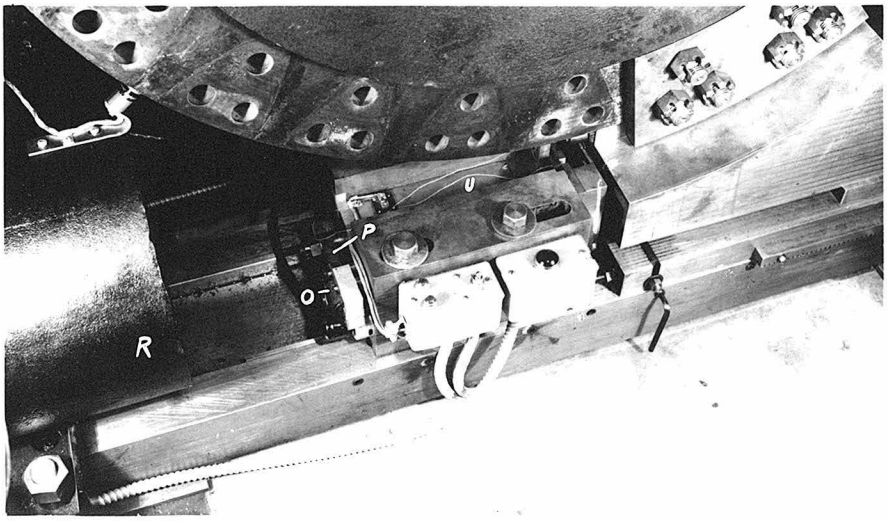

2. Specimens.--The unnotched specimens are machined from 1/2 inch diameter rod. They are threaded at each end and have a cylindrical gage length of 1.00 ± 0.005 inch, and a gage diameter of 0.200 ± 0.001 inch, as shown at K in Figure 12 and in the accompanying sketch, Figure 15. One end of the specimen screws into the end of the holder as at L, Figures 9 and 10, and on the other end of the specimen is screwed a tup or 1 inch square piece of steel 1/2 inch thick, shown at M, Figures 9 and 12. Thus the specimen is held firmly in a horizontal position tangent to the under edge of the wheel in such a manner that the jaws of the disc, under normal rotation, clear the specimen and tup by a small amount (see Figure 10). After bringing the wheel up to any desired speed, shown by the speed indicator at N on the control panel (Figure 7). a trigger mechanism is operated by a solenoid O (Figure 11), synchronized with the disc rotation. Instantaneous tripping of the trigger is accomplished by thyratron action. This trigger, P, releases a torsional spring which raises a flat yoke (Q, Figures 8 and 10) behind the tup into the path of the striking jaws. This yoke engages both the tup and striking jaws, after which the specimen is pulled off in tension. One end of the specimen, together with tup and yoke, flies off tangent to the wheel and is deposited in a container full of cotton waste at R, Figure 11.

3. Dynamometer.--The dynamometer for measuring forces during impact, shown at E in Figures 8 and 9, consists of a hollow cylindrical bar of S.A.E. 4140 steel, 13/16 inches in outer diameter, and 7/8 inches over-all length. It is threaded internally at the open end with 20 threads per inch, into which one end of the specimen may be

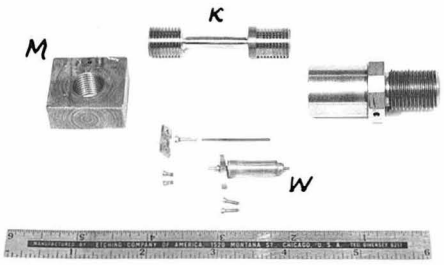


Fig. 12
Specimen, Dynamometer
Extensometer, tup (details)

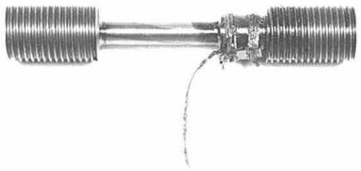

Fig. 13 Specimen-type strain gage

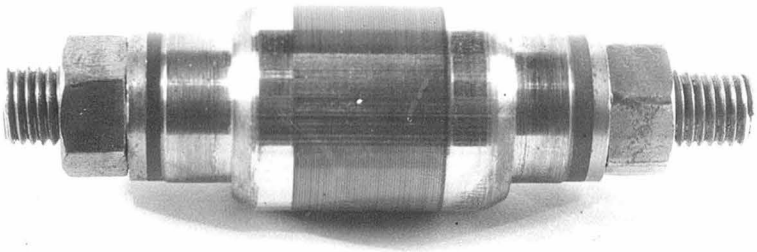

Fig. 14 Preliminary Design of Extensometer Core

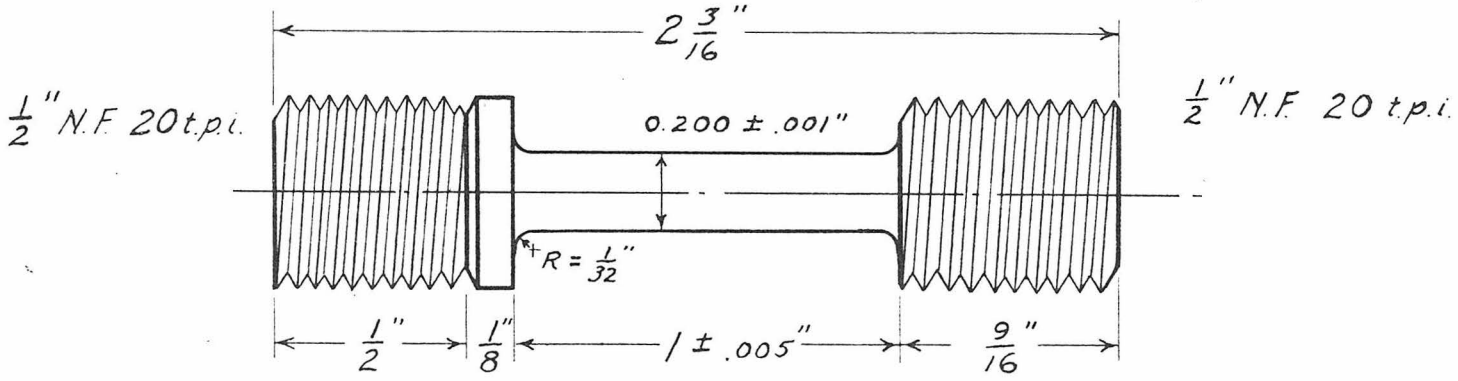


Note: Threads must be standard, right-hand.

Calif. Institute of Technology
Impact Research

TENSION SPECIMENS

Scale: Twice Full Size.

Fig. 15.

screwed. The other end of the dynamometer fastens rigidly into the anvil, F. The strain gage winding is laid longitudinally along the outer surface of this cylinder, and consists of approximately 30 feet of number 40 constantan wire formed into a mat in zig-zag fashion, coated with Glyptal as an insulating binder and baked at 250 degrees Fahrenheit. For purpose of protection, the wire is covered with scotch tape as shown at S, Figure 10. This constantan winding is referred to as the "pick-up" resistor.

The leads from this pick-up on the dynamometer are connected to the electric circuit shown in Figure 16. This circuit consists of a 140 volt battery, a series resistor placed in series with the pick-up, and a calibration resistor for purposes of calibrating the force measurements of the dynamometer as discussed later. The resistance of the series resistor is made very high compared to any change in the pick-up resistor during impact, so that a constant current of approximately 100 milliamperes is maintained in the circuit.

When a tension impact force acts on the specimen, it is transmitted through the specimen to the dynamometer, which elongates elastically in proportion to this force according to Hooke's Law. The wire covering the dynamometer bar follows this increase in length, changing its resistance in a linear manner in proportion to the force acting. Numerous tests, of which the data in Table I are typical, indicate that the change in resistance varies linearly with the load over a range of forces exceeding that used in any tension tests. With high strength steel specimens, 6000 pounds is ordinarily the maximum force which will occur.

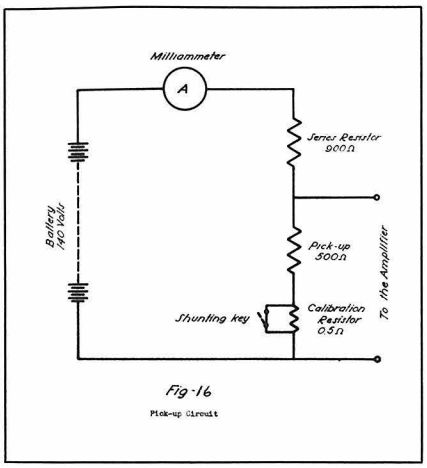


Fig. 16
Electrical Circuit

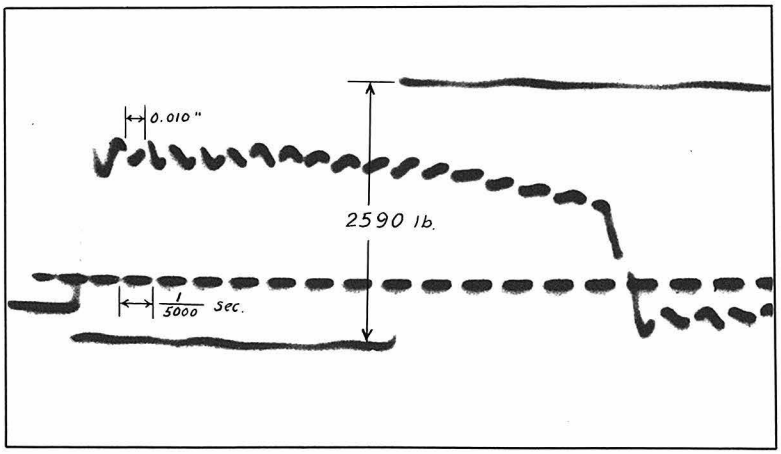


Fig. 17
Force-time-elongation diagram,
showing calibration curves for force and time

Aluminum specimen
20 feet per second
5 kilocycle timing-wave

TABLE I

Typical Pick-up Calibration Data

| Total Load pounds | Total Resistance ohms | Resistance Change ohms |
|---|---|---|
| 0 | 848.080 | |
| | | 0.430 |
| 2,000 | 848.510 | |
| | | 0.434 |
| 4,000 | 848.944 | |
| | | 0.446 |
| 6,000 | 849.390 | |
| | | 0.458 |
| 8,000 | 849.848 | |
| | | 0.412 |
| 10,000 | 850.260 | |
| | | 0.428 |
| 12,000 | 850.688 | |
| | | 0.438 |
| 10,000 | 850.250 | |
| | | 0.442 |
| 8,000 | 849.808 | |
| | | 0.438 |
| 6,000 | 849.370 | |
| | | 0.435 |
| 4,000 | 848.935 | |
| | | 0.425 |
| 2,000 | 848.510 | |
| | | 0.417 |
| 0 | 848.093 | |

Up to 12,000 pounds and back to zero load, as fast as possible (within 10 seconds), gives:

0 848.093

12,000, held for 10 minutes: 850.724 ohms, with no visible change.

6,000, held for 10 minutes: 849.410 ohms, with no visible change.

0 848.080

Results: Average resistance change: 2.180 ohms per 10,000 pounds, or 4585 pounds force per ohm change in resistance.

It is to be noted that the resistance for loading and unloading agree, within small limits of experimental error, indicating that the Glyptal binder is sufficiently strong to permit the wire of the pick-up to follow the change in length of the dynamometer under load. By measuring the change in voltage produced by this change in the resistance of the pick-up circuit, the forces can be determined as indicated later.

The linear relation between the impact forces and the dynamometer deformations is valid as long as the period of the natural vibration of the dynamometer bar is short compared with the duration of impact. The natural frequency of the dynamometer developed in this work is 35,000 cycles per second, which gives a time for a half period of 1/70,000 second. This is practically the upper limit of frequency for this type of dynamometer bar, since further shortening of the bar is impractical. The natural frequency is determined by striking the end of the dynamometer and comparing the vibrations set up on an oscillograph screen with a wave of known frequency. With this dynamometer, reliable force-time records are available up to impact speeds of 200 feet per second.

4. Recording Apparatus.--The voltage changes in the circuit produced by the elastic deformation of the dynamometer are amplified by a two-stage alternating current amplifier. From the amplifier the signal is sent to an RCA TM-168-A cathode ray oscillograph, shown at J in Figure 7. The connections are made such that the voltage changes will produce a vertical deflection of the electron beam. The scale for the vertical deflection in terms of resistance (ohms per inch) is determined by suddenly changing the resistance of the dynamometer

circuit a known amount. For this purpose, the calibration resistor shown in Figure 16 is used to produce a force-calibration curve after each test. The change in resistance of the dynamometer winding for given loads may be determined statically in a tension testing machine, as shown in Table I.

The circuit of the oscillograph is arranged so that a single horizontal sweep of the electron beam can be obtained at any desired speed. The sweep speed is determined by connecting a known frequency to the oscillograph, and producing a broken timing across the screen after each test.

This force-time curve traced by the beam on the screen of the oscillograph is recorded photographically with the camera shown at T in Figure 7. The camera is equipped with a Zeiss Biotar f:1.4 lens.

The horizontal single sweep of the oscillograph beam is started across the screen slightly in advance of the impact of jaws on tup by means of a small firing pin projecting beyond the front surface of the yoke. This pin is insulated from the yoke and connected through the wire shown at U, Figure 11, to a condenser in the control panel shown at V in Figure 7. The other side of the condenser is connected to ground. When the jaws of the disc strike the end of the pin the condenser is discharged, thereby starting the sweep of the electron beam. An instant later the hammers strike the tup, producing a force-time diagram in the center of the oscillograph screen.

5. Extensometer.—The picture photographed from the oscillograph screen is essentially a force-time diagram, with ordinates proportional to force and abscissas proportional to time. Units of

elongation may be added to the same diagram by means of a small extensometer, a preliminary model of which is shown in Figure 14. In final design, it consists of a small cylinder, 1/4 inch in diameter and one inch long, mounted on the end of the dynamometer parallel to and above the specimen gage length, as in Figures 9 and 10. This cylinder consists of 115 alternate layers of 0.009 inch celluloid and 0.001 inch aluminum foil, pressed onto a central steel shaft in such a manner that the aluminum discs make electrical contact with the central shaft (see W, Figure 12). The outer surface of the cylinder is turned smooth in a lathe. A narrow ribbon of clock-spring steel, carrying a needle point at one end, is fastened firmly to the tup prior to fracture of the specimen; this ribbon is held along an element of the cylinder by an elastic rubber tube. Figure 12 shows the parts, which are assembled in place as in Figure 9. As the tup is drawn forward during deformation of a specimen, the needle point scratches the surface of the cylinder, alternately making and breaking an electric circuit after every 0.010 inch of elongation. This produces successive modulations on the force-time diagram, corresponding to deformation units of 0.010 inch. Such modulations are shown in Figure 17 for aluminum, broken at 20 feet per second.

Investigation of these and similar diagrams indicates that the velocity of the wheel during impact is essentially constant, since equal units of elongation are marked out in equal time intervals. In addition, elongation measurements obtained with the extensometer check sufficiently close with those based on the assumption that the rate of deformation during fracture is constant and equal to the velocity of

the jaws. Consequently this extensometer device is used only occasionally as a check on the operation of the dynamometer-oscillograph unit.

Table II shows a few typical values of elongation measured from specimens and compared with corresponding values recorded from the photographed curves. The time required for fracture is also given. It is interesting to point out that with 20 per cent elongation, or 2/10 inch deformation up to fracture, the time required for fracture at 150 feet per second is 0.00011 second, or 1/9,000 second. Also, 150 feet per second corresponds to 180,000 per cent elongation per second.

TABLE II

Elongation-Time Results

| Specimen | Velocity ft./sec. | Measured Elongation in. | Elongation taken from Curves, in. | Time for Fracture sec. |
|---|---|---|---|---|
| Cold Drawn Steel #8 | 10 | 0.150 | 0.15 | 0.00125 |
| Cold Drawn Steel #17 | 10 | 0.157 | 0.155 | 0.00130 |
| Cold Drawn Steel #10 | 30 | 0.185 | 0.165 | 0.00049 |
| Cold Drawn Steel #16 | 50 | 0.145 | 0.15 | 0.00025 |
| Cold Drawn Steel #1 | 75 | 0.120 | 0.12 | 0.00013 |
| Brass #1 | 20 | 0.250 | 0.24 | 0.00104 |
| 17ST Duralumin #15 | 20 | 0.250 | 0.245 | 0.00104 |

B. Stress-Strain Relations under Impact Loading.

1. Materials Tested.--Using the procedure outlined above, between ten and twenty specimens of each of eight different engineering materials were prepared and broken in tension impact. With each material, tests were performed at velocities ranging from static conditions to rates of deformation of 150 feet per second or more. The materials tested were as follows:

(a) S.A.E. 1112 Free Cutting Steel, cold drawn.

(b) S.A.E. 1035 Steel, fully annealed.

(c) 16% Cr - 2% Ni Stainless Steel, oil quenched from 1800 degrees Fahrenheit:

(1) drawn at 1200 degrees Fahrenheit

(2) drawn at 900 degrees Fahrenheit

(3) drawn at 700 degrees Fahrenheit.

(d) 18% Cr - 8% Ni Stainless Steel.

(e) Rolled Silicon Bronze (Herculoy), 96.25% Cu, 3.25% Si, 0.50% Tin.

(f) 17ST Duralumin.

(g) 24ST Aluminum Alloy.

(h) Dow Metal X, extruded.

Typical photographs of the force-time curves as photographed on the oscillograph screen are shown in Figure 18 for the 16% Cr - 2% Ni Stainless Steel drawn at 1200 degrees Fahrenheit, for Silicon Bronze, and for 17ST Duralumin.

Such curves are photographically enlarged, and traced at a suitable size by drawing a mean line through the vibrations of the

diagram, after which the force, time, and elongation scales are determined. Successive force measurements and corresponding elongations may be recorded in suitable units, and the areas under the curves measured with a planimeter. Knowing the initial cross-sectional area and length of each specimen, stress-strain values are computed, and the curves plotted. The energy required to rupture the specimen is obtained directly from the area of the force-elongation curve. For purposes of comparison, static tests were made with each material, and corresponding data obtained.

2. Analysis of Test Records.--A complete analysis of the stress-strain curve for 17ST Duralumin broken at 51 feet per second is carried out in Figure 19, and the results are tabulated in Table III.

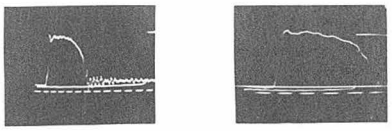

35'/sec. 75'/sec.

16% Cr.-2% Ni. Stainless Steel,
Oil Quenched 1800°F., Tempered 1200°F.

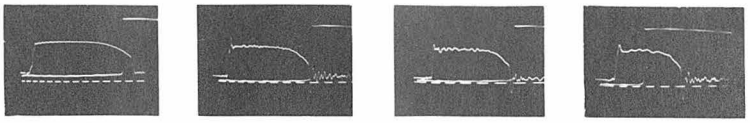

10'/sec. 38'/sec. 53'/sec. 90'/sec.

Rolled Silicon Bronze

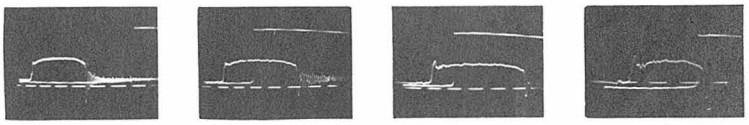

30'/sec. 50'/sec. 70'/sec. 147'/sec.

17 ST Duralumin

Fig. 18
Typical Force-time Diagrams

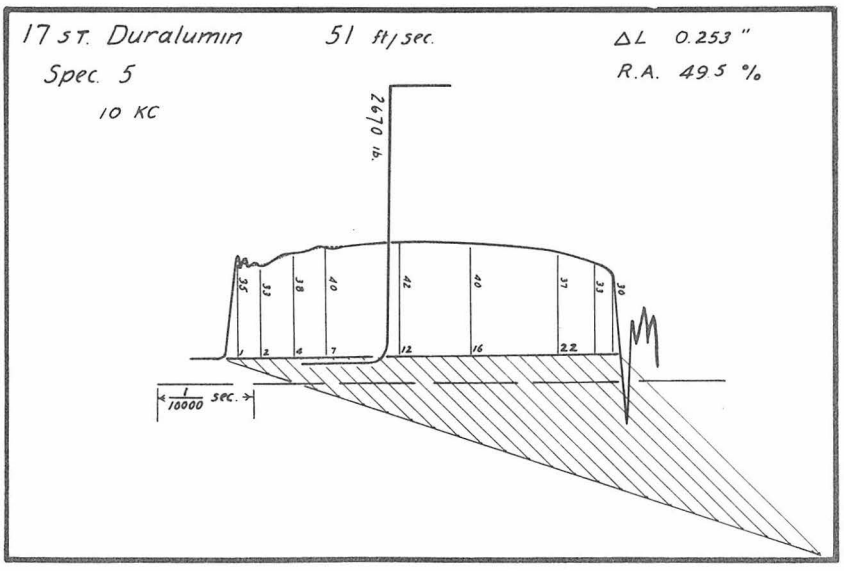


Fig. 19
Typical Analysis
of Enlarged Force-time Diagram

## TABLE III

### Complete Analysis of Stress-Strain Curve of Figure 19

17ST Duralumin
Specimen: 5
Film Holder: 4
Timing Wave: 10 kilocycles

Original Sectional Area: $\frac{\pi}{100}$ sq.in.
% Elongation: 25.3
% Reduction of Area: 49.5

Planimeter Reading: 1.94
Planimeter Constant: 1.113
Area of Diagram: 2.160 sq.in.

Time of Break: 0.000416 sec.
Velocity: 50.5 ft./sec.

Energy of Rupture: 41.9 ft.lb.
Yield Stress: 59,400 p.s.i.
Ultimate Stress: 71,300 p.s.i.
Breaking Stress: 51,000 p.s.i.

Force Scale: 1 in. = 2670 lb.
Elongation Scale: 1 in. = 0.0727 ft.
Energy Scale: 1 sq.in. = 19.4 ft.lb.

| Elongation in./in. | Force Units (50ths of an inch) | Force lb. | Stress lb./sq.in. |
|---|---|---|---|
| 0.001 | 35 | 1870 | 59,400 |
| 0.002 | 33 | 1760 | 56,000 |
| 0.004 | 38 | 2030 | 64,500 |
| 0.007 | 40 | 2135 | 68,000 |
| 0.012 | 42 | 2240 | 71,300 |
| 0.016 | 40 | 2135 | 68,000 |
| 0.022 | 37 | 1975 | 62,700 |
| 0.024 | 33 | 1760 | 56,000 |
| 0.025 | 30 | 1600 | 51,000 |

## Chapter V

## Test Data and Results of This Investigation

In accordance with the above test procedure, representative values of yield stress, breaking stress and ultimate stress, when this last is distinct from the yield stress, are recorded in Tables IV to XI, for each material at various speeds of impact. Likewise the per cent elongation, reduction of area, and energy required to rupture the specimens are recorded. Ratios of the average dynamic to static values of yield strength, absorbed energy, per cent elongation, and reduction of area are plotted in Figures 20 to 23 respectively. For purposes of comparison of these properties, the materials are grouped into (a) ferrous and (b) non-ferrous alloys. Significant stress-strain curves for each material at pertinent rates of deformation are shown in Figures 24 to 33. Curves showing the variation of the physical properties with rates of deformation are shown in Figures 24a to 33a.

Due to the limited number of specimens available, these magnitudes of the physical properties are not considered to be definitely or exactly established within a range of plus or minus 5 per cent. However, the trends of these quantities are very pronounced, and it is believed they afford a basis for the following discussion.

A. For Tables IV to XI, see pages 37 to 41.

B. For Figures 20 to 33, see pages 42 to 68.

TABLE IV

Tensile Properties

S.A.E. 1112 Steel - Cold Drawn

| Velocity ft./sec. | Yield Stress p.s.i. | Ultimate Stress p.s.i. | Breaking Stress p.s.i. | Energy ft.lb. | Reduction of Area % | Elongation % |
|---|---|---|---|---|---|---|
| Static | 90,600 | 105,000 | 84,300 | 26.3 | 37.8 | 10.5 |
| 10 | 123,400 | ↑ | 85,000 | 46.5 | 40.6 | 16.0 |
| 24 | 135,200 | | 81,500 | 43.4 | 48.1 | 15.2 |
| 37 | 136,000 | not distinct | 86,500 | 44.5 | 47.5 | 15.2 |
| 53 | 143,500 | from | 90,000 | 53.0 | 52.4 | 18.2 |
| 80 | 150,000 | yield stress | 75,000 | 36.3 | 45.0 | 13.0 |
| 93 | 155,000 | | 91,000 | 47.1 | 43.8 | 14.5 |
| 145 | 160,000 | ↓ | 110,000 | 37.0 | 47.5 | 11.2 |
| 155 | 163,000 | | 114,000 | 42.8 | 44.0 | 13.0 |

TABLE V

Tensile Properties

S.A.E. 1035 Steel - Fully Annealed

| Velocity ft./sec. | Yield Stress p.s.i. | Ultimate Stress p.s.i. | Breaking Stress p.s.i. | Energy ft.lb. | Reduction of Area % | Elongation % |
|---|---|---|---|---|---|---|
| Static | 47,700 | 76,500 | 63,600 | 49.0 | 51.0 | 26.5 |
| 10 | 87,500 | 95,500 | 69,500 | 59.9 | 52.5 | 26.0 |
| 39 | 92,800 | 99,000 | 68,000 | 62.1 | 53.7 | 26.5 |
| 47 | 105,500 | 108,500 | 75,800 | 72.0 | 53.7 | 28.0 |
| 57 | 102,300 | 105,400 | 78,000 | 62.2 | 53.7 | 27.0 |
| 67 | 107,500 | 109,000 | 70,000 | 60.2 | 51.7 | 25.0 |
| 88 | 118,000 | 114,000 | 73,800 | 71.6 | 55.1 | 26.9 |
| 120 | 120,000 | 112,000 | 64,000 | 69.9 | 55.7 | 27.5 |
| 130 | 125,000 | 107,000 | 57,000 | 79.1 | 56.5 | 30.5 |
| 140 | 121,000 | 97,000 | 55,000 | 75.8 | 56.7 | 32.0 |

## TABLE VI

### Tensile Properties

### 16% Cr - 2% Ni Stainless Steel
### Oil Quenched 1800° F.

a: drawn 1200° F.
b: drawn 900° F.
c: drawn 700° F.

| | Velocity ft./sec. | Yield Stress p.s.i. | Ultimate Stress p.s.i. | Breaking Stress p.s.i. | Energy ft.lb. | Reduction of Area % | Elongation % |
|---|---|---|---|---|---|---|---|
| a | Static | 99,000 | 126,000 | 84,000 | 57.1 | 61.5 | 18.5 |
| b | Static | 204,000 | 215,000 | 143,000 | 110.0 | 63.5 | 21.0 |
| c | Static | 194,000 | 204,000 | 154,000 | 73.1 | 53.0 | 15.0 |
| a | 37 | 158,000 | 158,000 | 85,000 | 70.9 | 64.0 | 20.0 |
| b | 33 | 196,000 | 176,000 | 89,500 | 54.9 | 60.3 | 14.6 |
| c | 33 | 204,500 | 197,500 | 88,500 | 59.2 | 60.3 | 14.1 |
| b | 65 | 267,000 | 215,000 | 116,000 | 82.1 | 60.3 | 16.6 |
| c | 61 | 256,000 | 232,000 | 100,000 | 84.6 | 60.3 | 16.2 |
| a | 75 | 166,500 | 173,000 | 85,000 | 94.3 | 65.8 | 21.5 |
| b | 83 | 225,000 | 195,000 | 113,000 | 72.0 | 60.3 | 16.3 |
| c | 81 | 216,000 | 185,000 | 97,000 | 64.3 | 60.3 | 16.0 |
| a | 107 | 192,000 | 168,000 | 85,000 | 86.4 | 66.3 | 23.5 |
| b | 105 | 214,000 | 170,000 | 68,000 | 66.4 | 61.2 | 17.5 |
| c | 127 | 294,000 | 225,000 | 127,000 | 107.0 | 61.2 | 20.0 |

TABLE VII

Tensile Properties

18% Cr - 8% Ni Stainless Steel

| Velocity ft./sec. | Yield Stress p.s.i. | Ultimate Stress p.s.i. | Breaking Stress p.s.i. | Energy ft.lb. | Reduction Of Area % | Elongation % |
|---|---|---|---|---|---|---|
| Static | 44,000 | 97,500 | 88,000 | 163.0 | 70.3 | 72.0 |
| 5 | 70,000 | 111,000 | 79,000 | 116.8 | 63.4 | 44.0 |
| 9 | 70,400 | 117,000 | 92,000 | 127.8 | 64.0 | 45.5 |
| 22 | 77,000 | 127,000 | 103,000 | 154.3 | 61.5 | 51.6 |
| 49 | 95,000 | 131,000 | 109,000 | 164.5 | 60.3 | 52.0 |
| 73 | 106,500 | 127,500 | 109,000 | 182.0 | 59.0 | 56.2 |
| 90 | 102,000 | 119,000 | 86,500 | 148.8 | 60.3 | 52.0 |
| 106 | 98,000 | 117,000 | 87,000 | 145.8 | 61.5 | 53.2 |
| 143 | 124,000 | 130,500 | 104,000 | 153.7 | 61.5 | 50.0 |

TABLE VIII

Tensile Properties

Rolled Silicon Bronze

| Velocity ft./sec. | Yield Stress p.s.i. | Ultimate Stress p.s.i. | Breaking Stress p.s.i. | Energy ft.lb. | Reduction Of Area % | Elongation % |
|---|---|---|---|---|---|---|
| Static | 71,600 | 73,100 | 37,600 | 36.0 | 79.0 | 21.3 |
| 10 | 92,000 | 95,100 | 52,400 | 63.5 | 76.4 | 27.7 |
| 22 | 95,600 | 99,000 | 46,200 | 64.7 | 77.4 | 28.0 |
| 38 | 99,000 | 95,600 | 42,800 | 73.1 | 78.4 | 32.0 |
| 53 | 97,000 | 90,600 | 39,600 | 65.2 | 78.4 | 30.0 |
| 61 | 104,500 | 99,500 | 45,000 | 74.0 | 78.4 | 30.7 |
| 66 | 110,000 | 107,000 | 51,700 | 65.6 | 75.0 | 27.5 |
| 75 | 100,000 | 98,250 | 44,400 | 75.5 | 78.4 | 34.0 |
| 89 | 97,600 | 93,000 | 38,000 | 70.3 | 77.0 | 33.5 |
| 120 | 105,500 | 99,000 | 33,000 | 83.0 | 78.0 | 38.0 |
| 148 | 114,000 | 98,000 | 25,000 | 78.2 | 77.0 | 32.5 |
| 168 | 112,000 | 88,000 | 20,000 | 76.0 | 79.0 | 31.6 |
| 187 | 115,000 | 98,500 | 15,000 | 77.5 | 79.8 | 31.0 |

TABLE IX

Tensile Properties

17ST Duralumin

| Velocity ft./sec. | Yield Stress p.s.i. | Ultimate Stress p.s.i. | Breaking Stress p.s.i. | Energy ft.lb. | Reduction of Area % | Elongation % |
|---|---|---|---|---|---|---|
| Static | 31,800 | 54,700 | 44,500 | 30.7 | 45.2 | 23.0 |
| 11 | 45,700 | 58,600 | 45,600 | 34.0 | 49.0 | 23.8 |
| 16 | 51,600 | 66,200 | 51,700 | 38.2 | 46.0 | 24.1 |
| 31 | 56,000 | 67,600 | 51,100 | 40.5 | 51.0 | 25.3 |
| 51 | 59,400 | 71,300 | 51,000 | 41.9 | 49.5 | 25.3 |
| 70 | 57,800 | 68,000 | 45,900 | 41.0 | 52.4 | 25.8 |
| 109 | 60,500 | 65,200 | 45,600 | 40.5 | 53.0 | 27.5 |
| 139 | 66,000 | 62,500 | 35,500 | 40.9 | 54.5 | 28.3 |
| 147 | 72,000 | 72,000 | 45,500 | 48.0 | 55.3 | 28.1 |

TABLE X

Tensile Properties

24ST Aluminum Alloy

| Velocity ft./sec. | Yield Stress p.s.i. | Ultimate Stress p.s.i. | Breaking Stress p.s.i. | Energy ft.lb. | Reduction of Area % | Elongation % |
|---|---|---|---|---|---|---|
| Static | 46,000 | 65,600 | 64,000 | 32.0 | 33.0 | 20.0 |
| 10 | 56,000 | 73,000 | 63,000 | 35.7 | 32.7 | 20.2 |
| 37 | 67,100 | 77,800 | 65,400 | 43.0 | 40.6 | 22.3 |
| 64 | 75,000 | 81,800 | 70,000 | 46.0 | 36.8 | 23.5 |
| 89 | 71,300 | 76,100 | 63,400 | 40.4 | 40.0 | 22.0 |
| 117 | 79,600 | 78,000 | 61,500 | 46.0 | 41.5 | 24.8 |
| 148 | 84,800 | 78,000 | 61,500 | 46.6 | 41.0 | 25.0 |

TABLE XI

Tensile Properties

Dow Metal X

| Velocity ft./sec. | Yield Stress p.s.i. | Ultimate Stress p.s.i | Breaking Stress p.s.i | Energy ft.lb. | Reduction of Area % | Elongation % |
|---|---|---|---|---|---|---|
| Static | 30,000 | 39,000 | 34,000 | 13.0 | 39.8 | 14.4 |
| 10 | 45,600 | 45,600 | 33,000 | 16.9 | 46.7 | 15.4 |
| 33 | 49,000 | 49,000 | 32,000 | 14.8 | 46.0 | 14.5 |
| 70 | 61,300 | 51,000 | 33,000 | 21.2 | 45.3 | 17.0 |
| 110 | 62,000 | 46,000 | 29,000 | 22.6 | 45.3 | 19.2 |
| 135 | 67,000 | 51,500 | 34,500 | 21.9 | 42.0 | 17.5 |

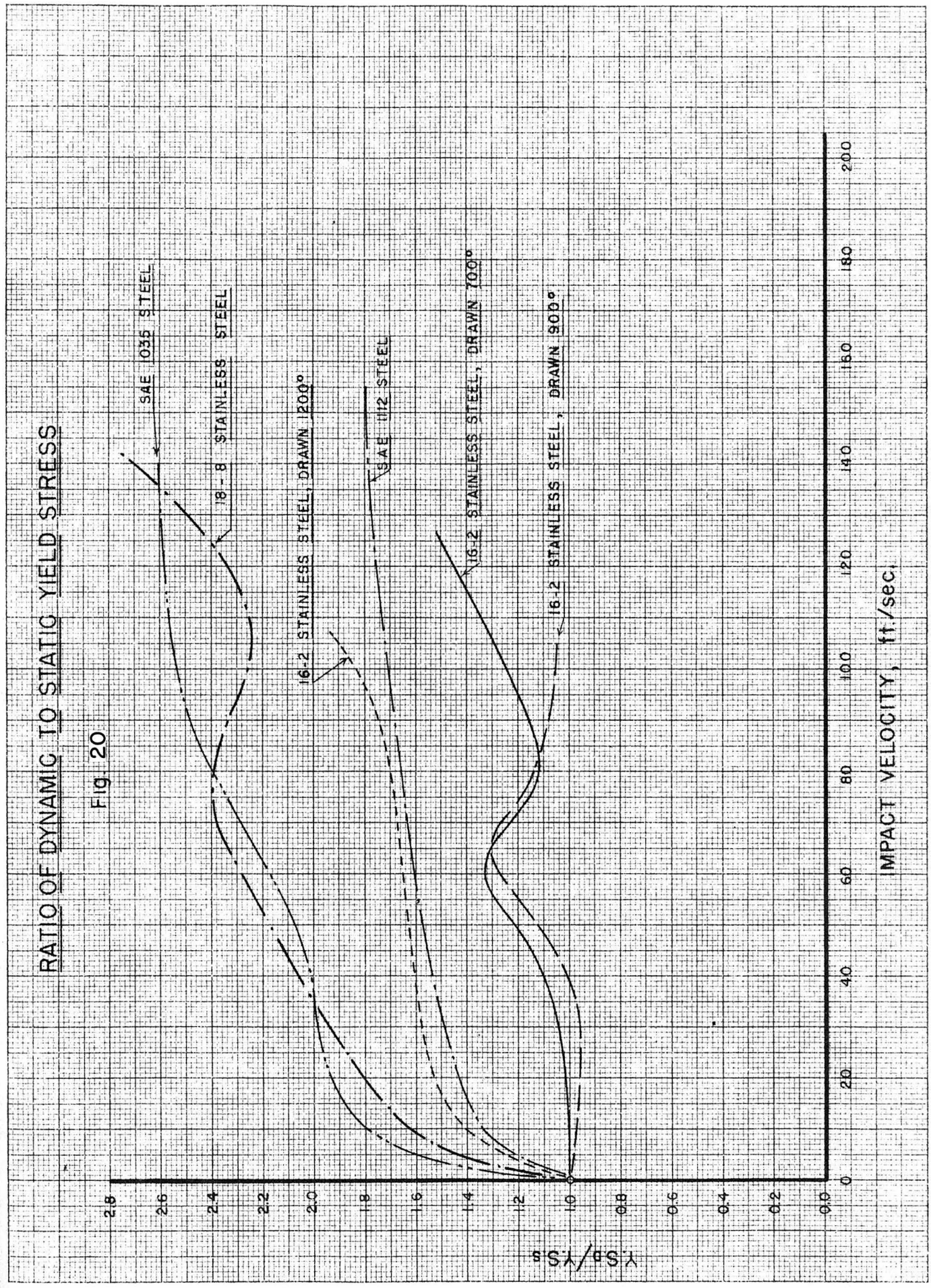
RATIO OF DYNAMIC TO STATIC YIELD STRESS
SAE 035 STEEL
18-8 STAINLESS STEEL
16-2 STAINLESS STEEL, DRAWN 1200°
SAE 1112 STEEL
16-2 STAINLESS STEEL, DRAWN 700°
16-2 STAINLESS STEEL, DRAWN 900°
$\gamma_d S_d / \gamma_s S_s$
IMPACT VELOCITY, ft./sec.
0.0
0.2
0.4
0.6
0.8
1.0
1.2
1.4
1.6
1.8
2.0
2.2
2.4
2.6
2.8
0
20
40
60
80
100
120
140
160
180
200

Fig. 20

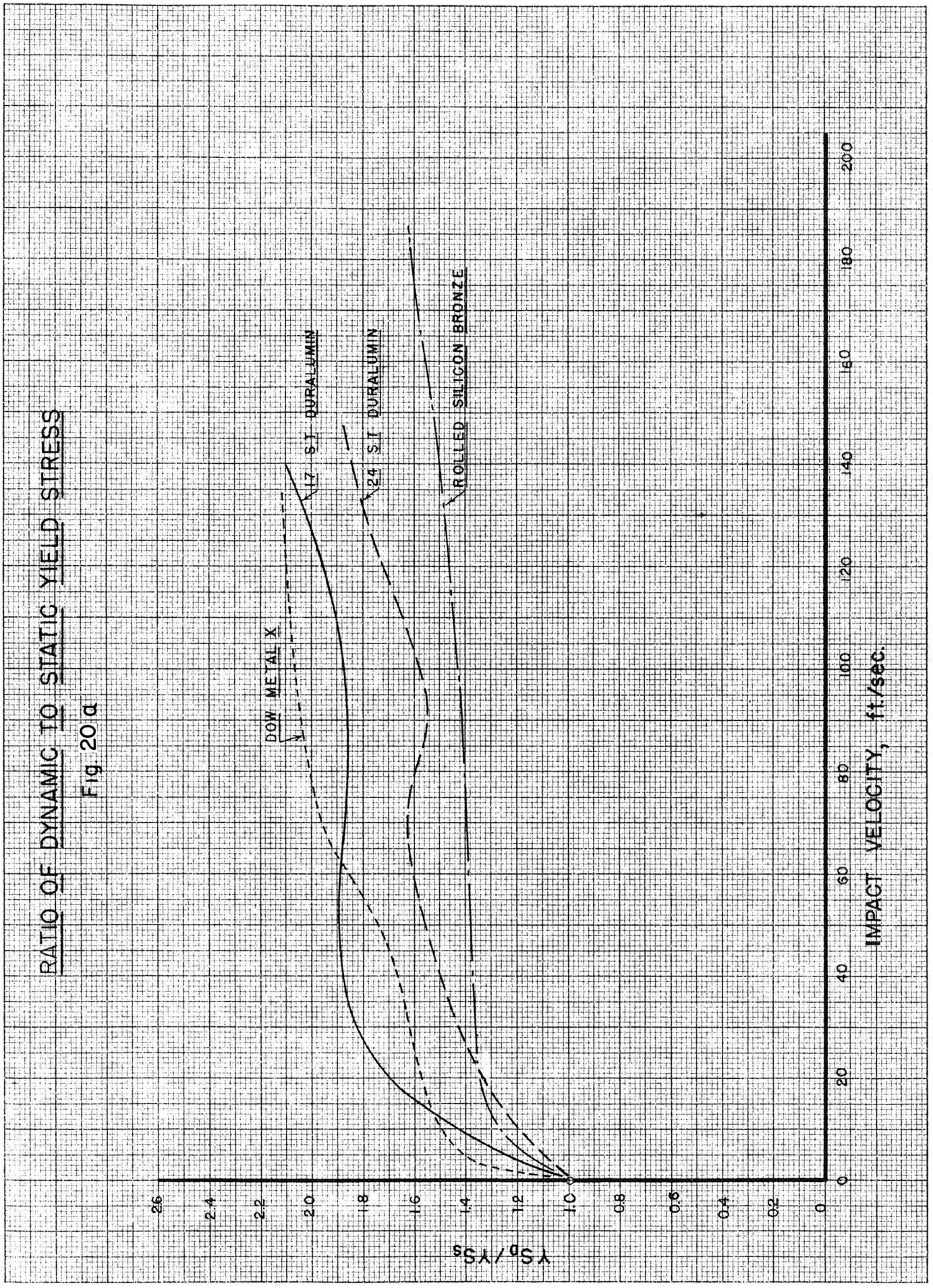
RATIO OF DYNAMIC TO STATIC YIELD STRESS
Fig 20a
DOW METAL X
17 S.T DURALUMIN
24 S.T DURALUMIN
ROLLED SILICON BRONZE
$\gamma S_D / \gamma S_S$
IMPACT VELOCITY, ft./sec.
0
0.2
0.4
0.6
0.8
1.0
1.2
1.4
1.6
1.8
2.0
2.2
2.4
2.6
0
20
40
60
80
100
120
140
160
180
200

RATIO OF DYNAMIC TO STATIC ENERGY ABSORBED

Fig. 21

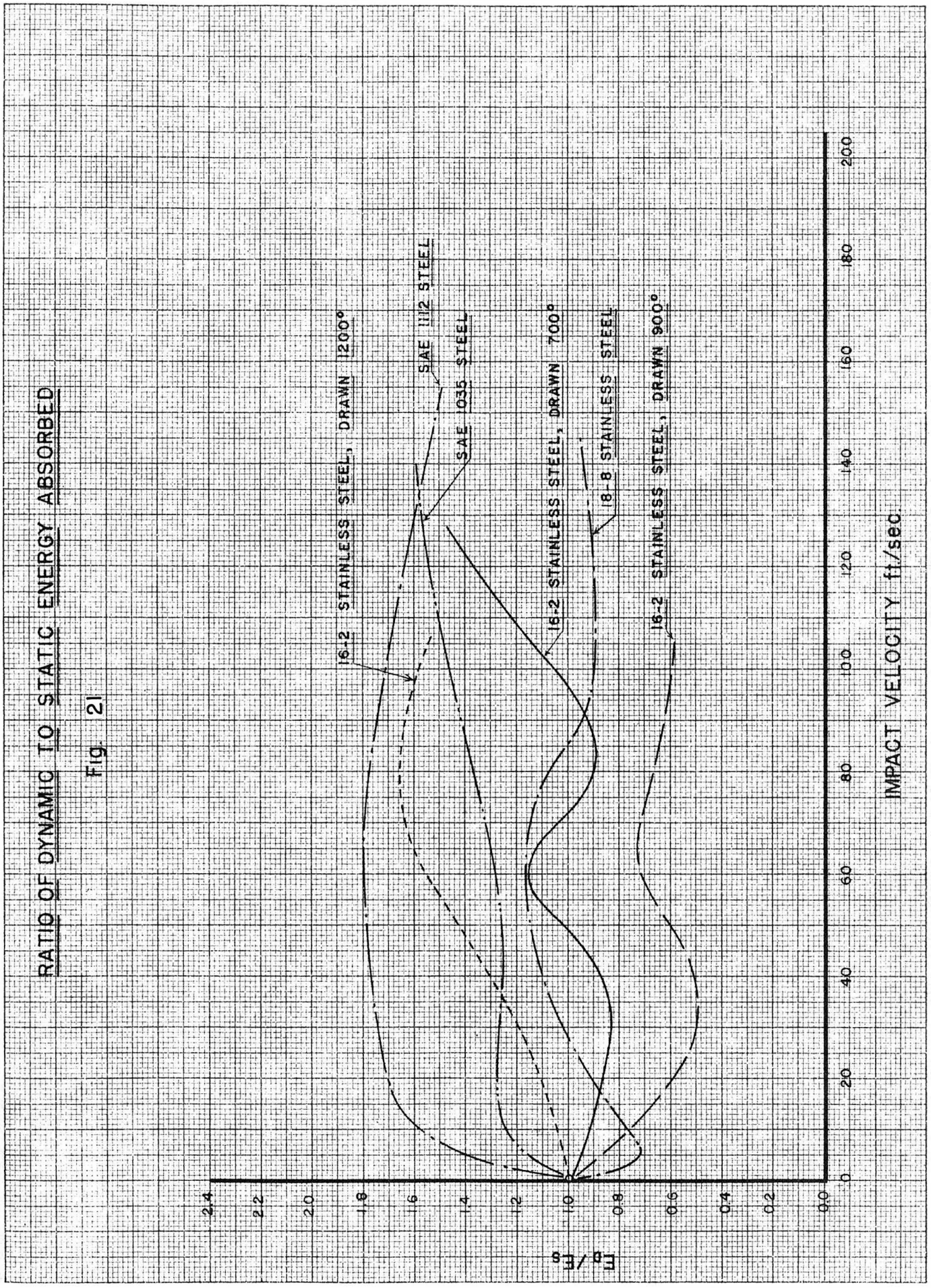

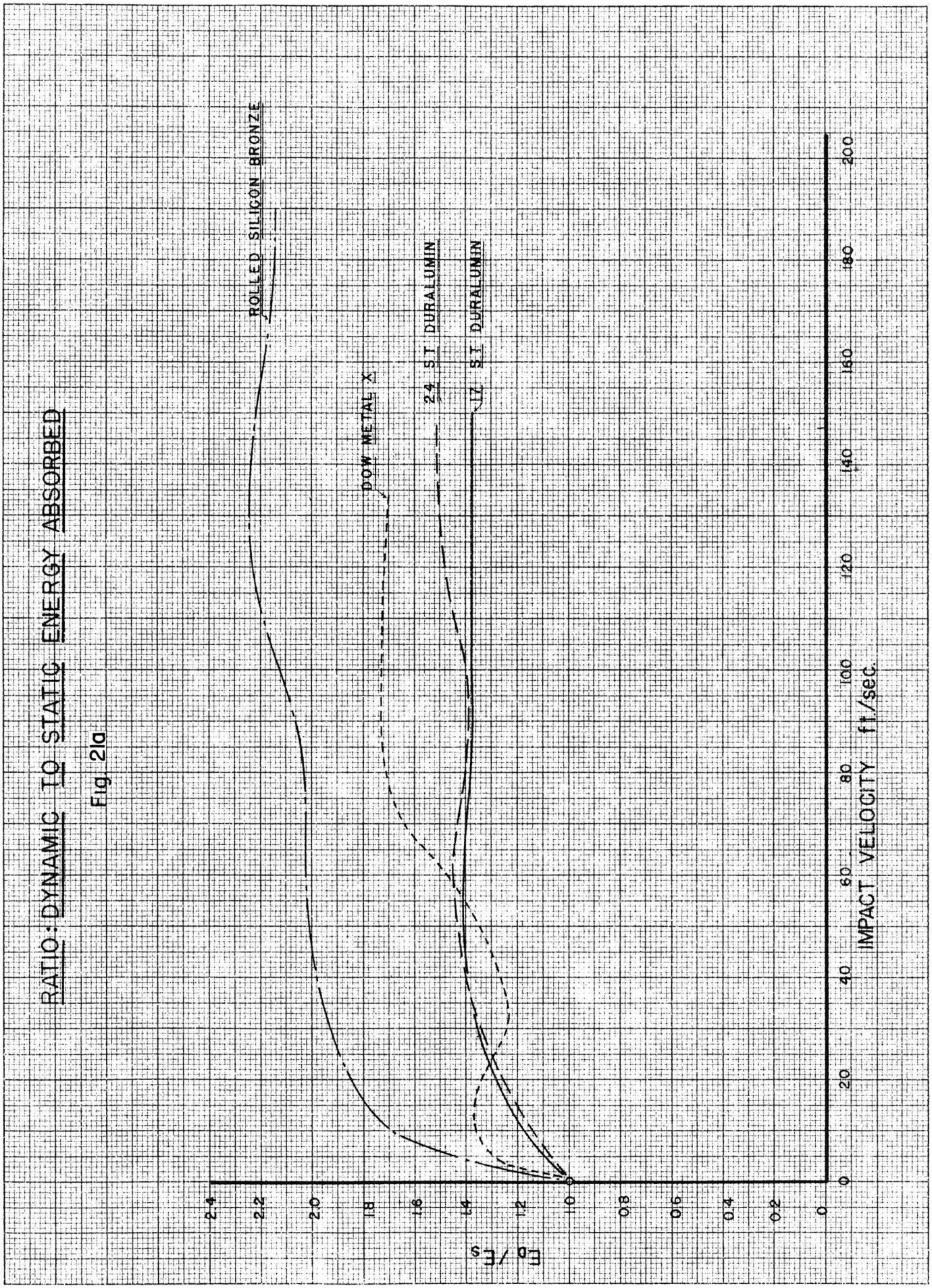
RATIO: DYNAMIC TO STATIC ENERGY ABSORBED
Fig. 21a
ROLLED SILICON BRONZE
DOW METAL X
24 S.T DURALUMIN
17 S.T DURALUMIN
$E_d / E_s$
IMPACT VELOCITY ft./sec.
0
0.2
0.4
0.6
0.8
1.0
1.2
1.4
1.6
1.8
2.0
2.2
2.4
0
20
40
60
80
100
120
140
160
180
200

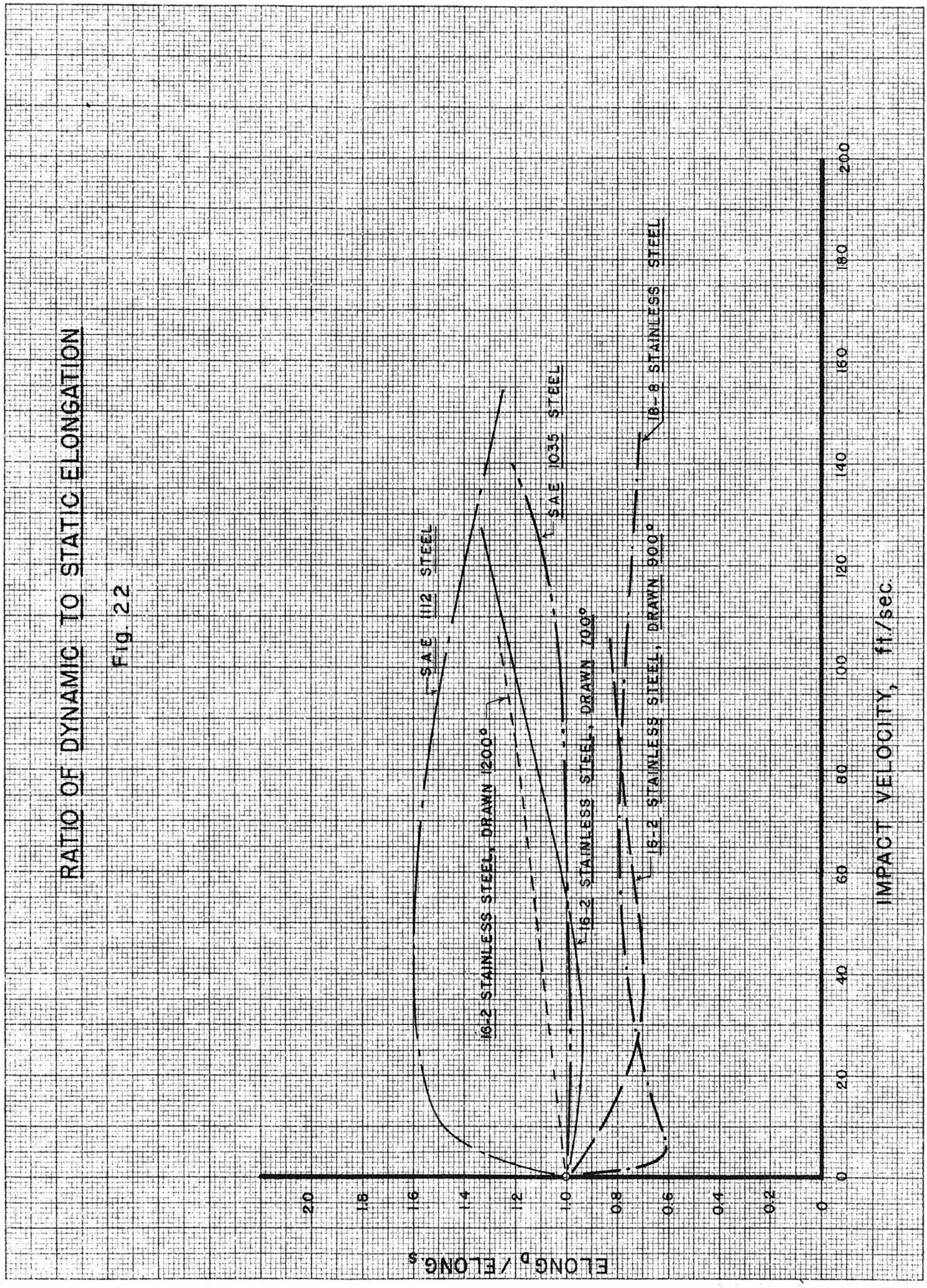
RATIO OF DYNAMIC TO STATIC ELONGATION
Fig. 22
ELONG$_D$ / ELONG$_S$
IMPACT VELOCITY, ft./sec.
0
0.2
0.4
0.6
0.8
1.0
1.2
1.4
1.6
1.8
2.0
0
20
40
60
80
100
120
140
160
180
200
SAE 1112 STEEL
SAE 1035 STEEL
18-8 STAINLESS STEEL
16-2 STAINLESS STEEL, DRAWN 1200°
16-2 STAINLESS STEEL, DRAWN 700°
16-2 STAINLESS STEEL, DRAWN 900°

# RATIO OF DYNAMIC TO STATIC ELONGATION

Fig. 22 a

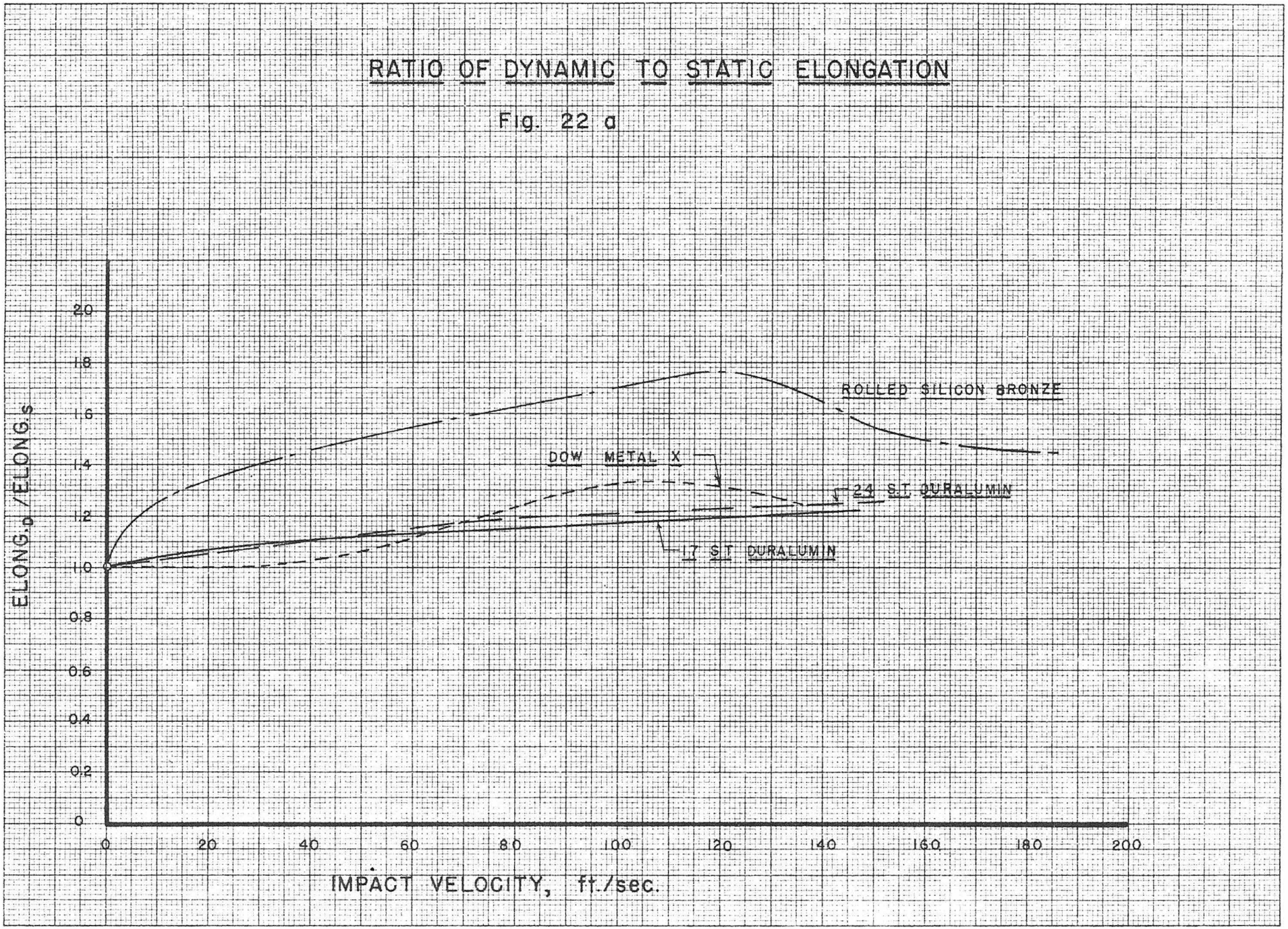

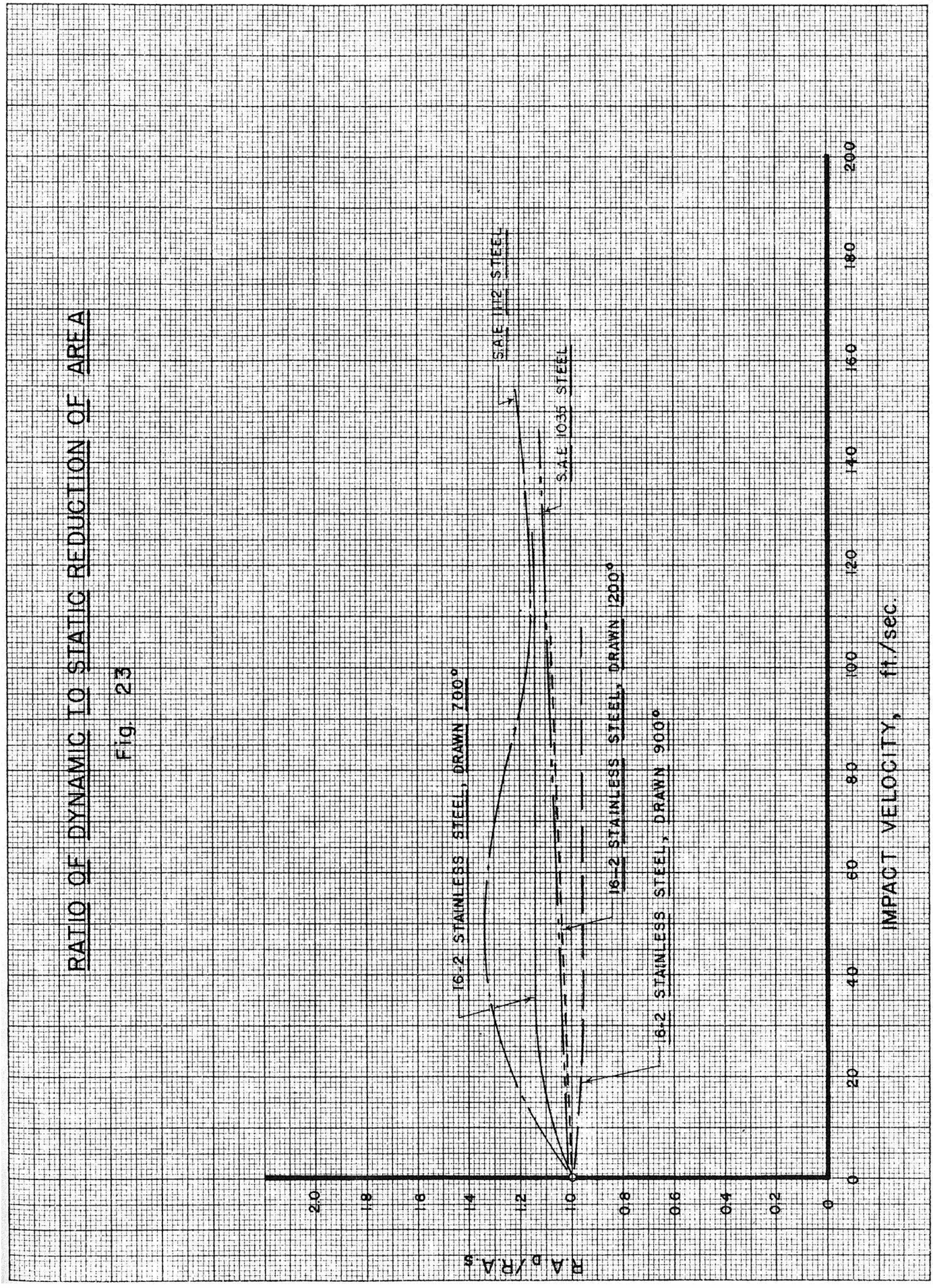
RATIO OF DYNAMIC TO STATIC REDUCTION OF AREA
Fig. 23
R_d/R_s
2.0
1.8
1.6
1.4
1.2
1.0
0.8
0.6
0.4
0.2
0
0
20
40
60
80
100
120
140
160
180
200
IMPACT VELOCITY, ft./sec.
16-2 STAINLESS STEEL, DRAWN 700°
S.A.E. 1112 STEEL
S.A.E. 1035 STEEL
16-2 STAINLESS STEEL, DRAWN 200°
16-2 STAINLESS STEEL, DRAWN 900°

RATIO OF DYNAMIC TO STATIC REDUCTION OF AREA

Fig. 23a

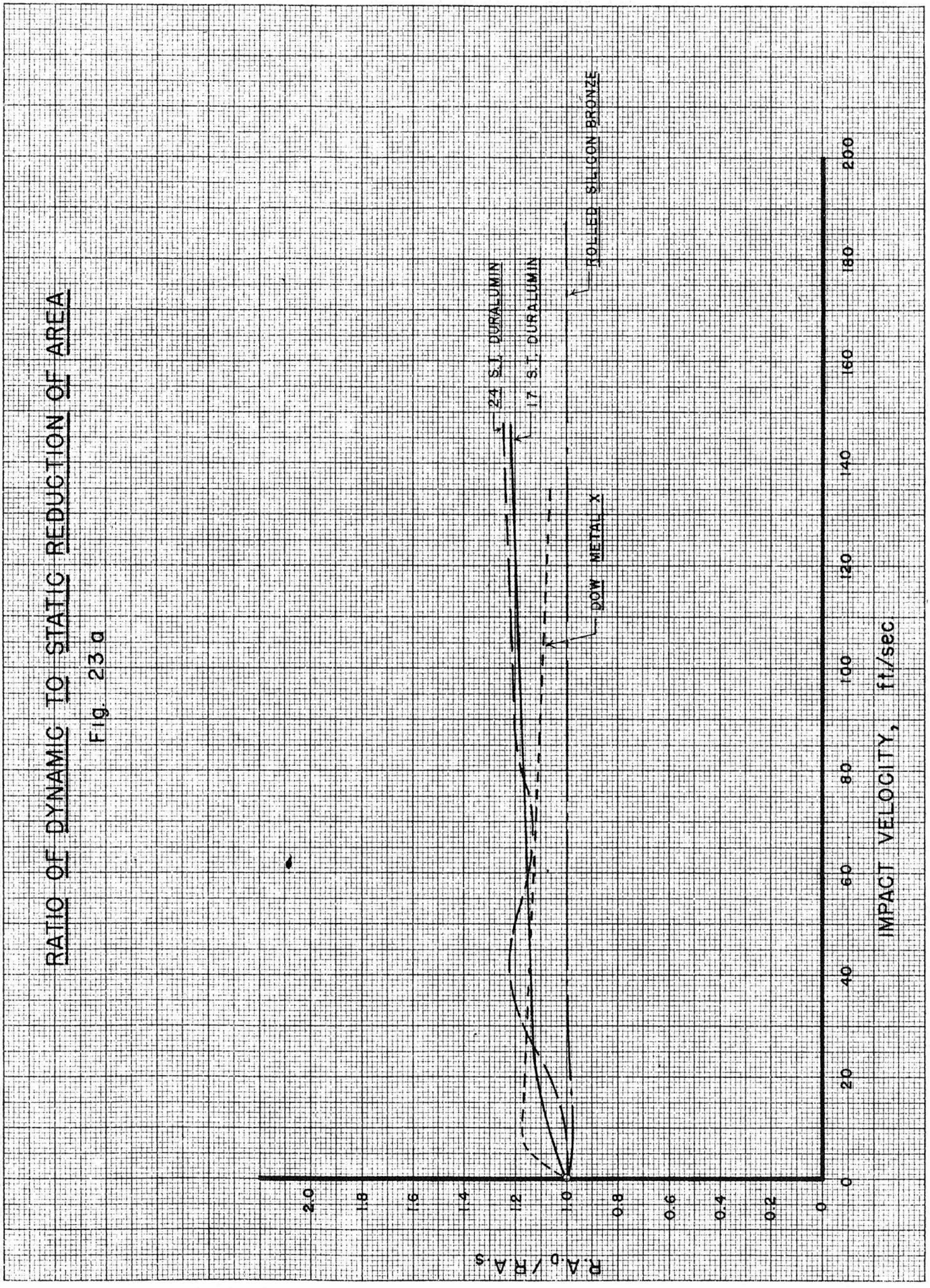

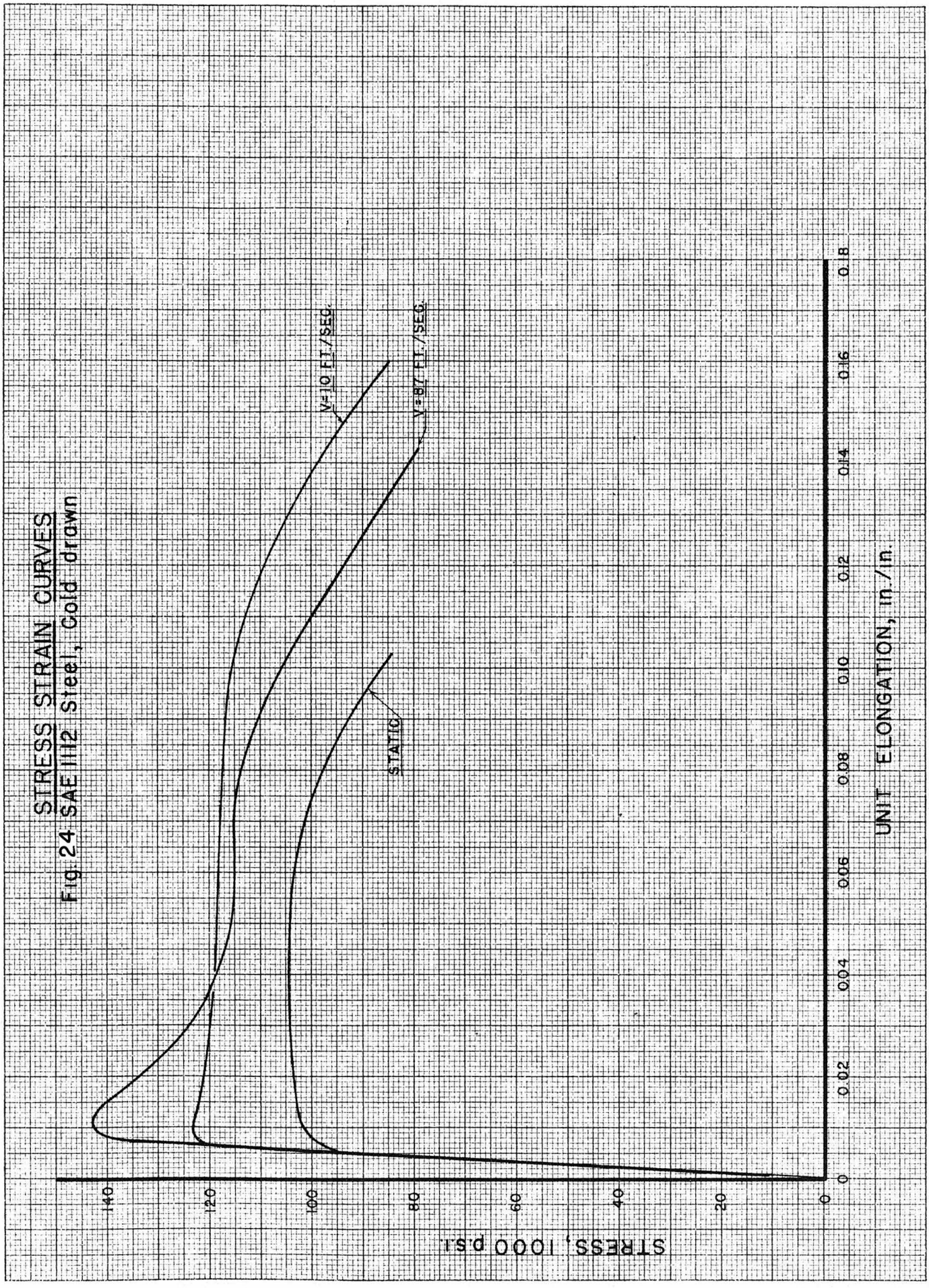
STRESS STRAIN CURVES
Fig. 24 SAE 1112 Steel, Cold drawn
V=10 FT./SEC.
V=87 FT./SEC.
STATIC
STRESS, 1000 p.s.i.
UNIT ELONGATION, in./in.
0
20
40
60
80
100
120
140
0.02
0.04
0.06
0.08
0.10
0.12
0.14
0.16
0.18

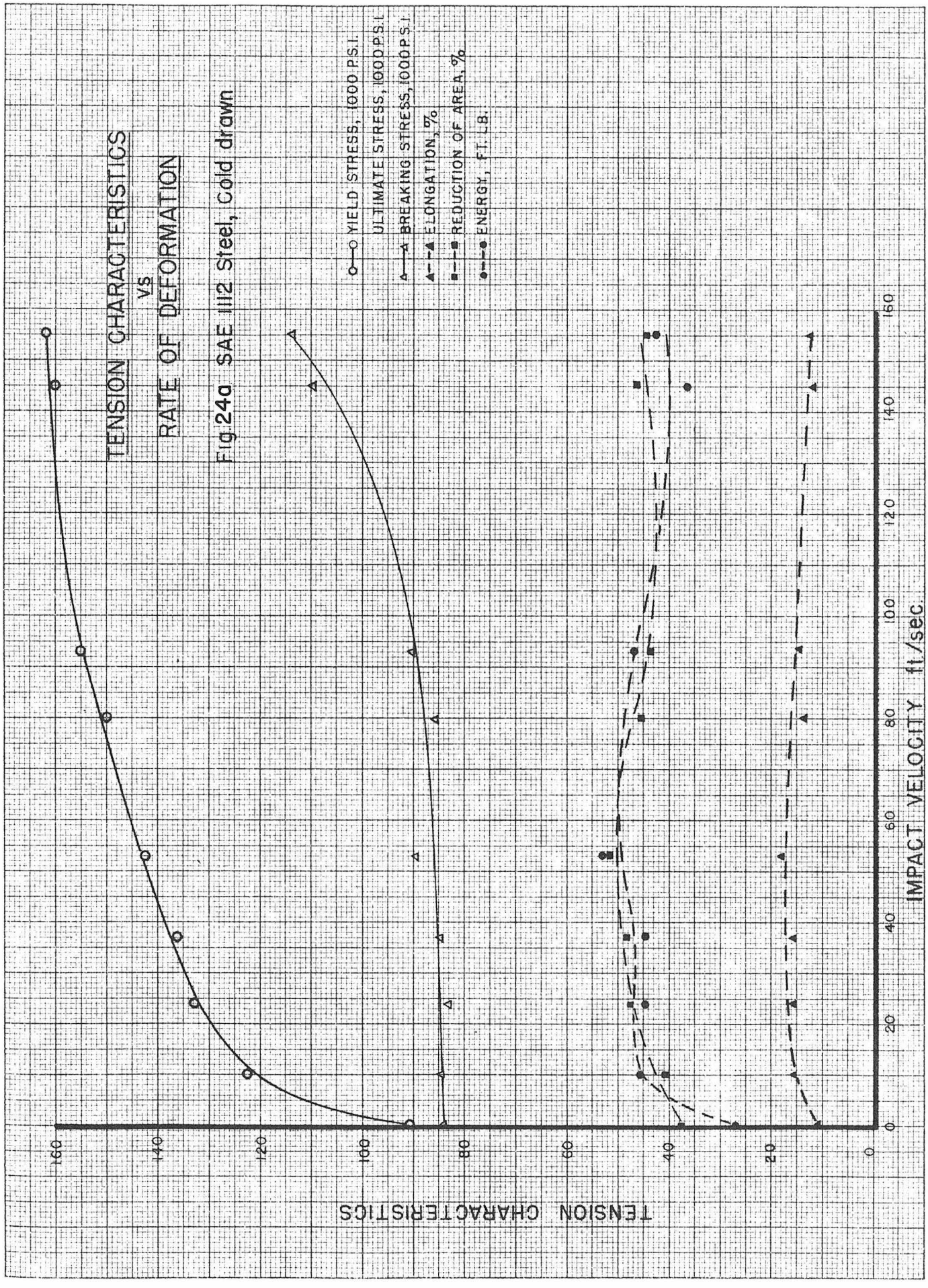
TENSION CHARACTERISTICS
vs
RATE OF DEFORMATION
Fig. 24a SAE 1112 Steel, Cold drawn
YIELD STRESS, 1000 P.S.I.
ULTIMATE STRESS, 1000 P.S.I.
BREAKING STRESS, 1000 P.S.I.
ELONGATION, %
REDUCTION OF AREA, %
ENERGY, FT. LB.
TENSION CHARACTERISTICS
IMPACT VELOCITY ft./sec.
0
20
40
60
80
100
120
140
160

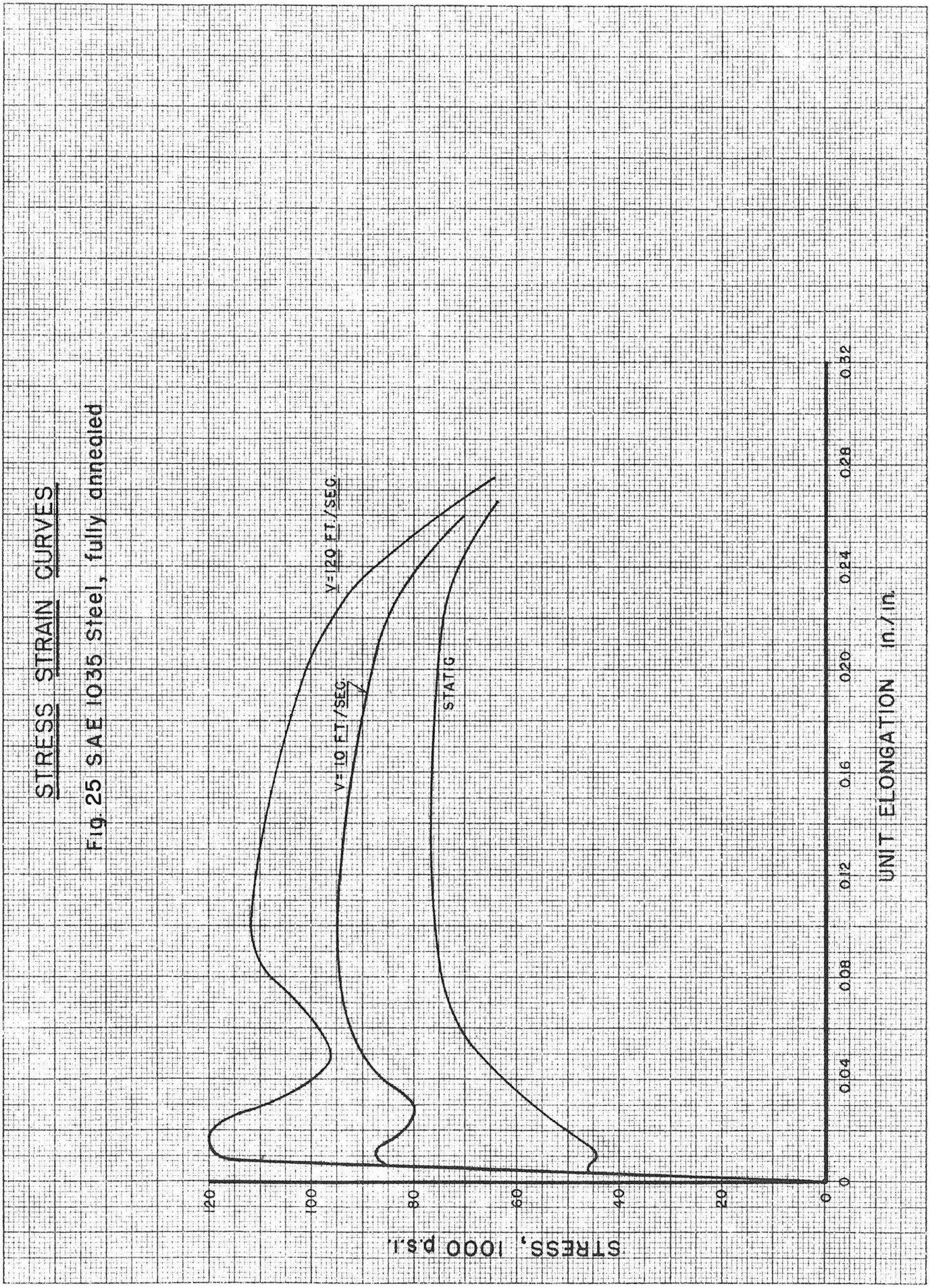
STRESS STRAIN CURVES
Fig 25 SAE 1035 Steel, fully annealed
V=120 FT./SEC.
V=10 FT./SEC.
STATIC
STRESS, 1000 p.s.i.
UNIT ELONGATION in./in.
120
100
80
60
40
20
0
0.04
0.08
0.12
0.16
0.20
0.24
0.28
0.32

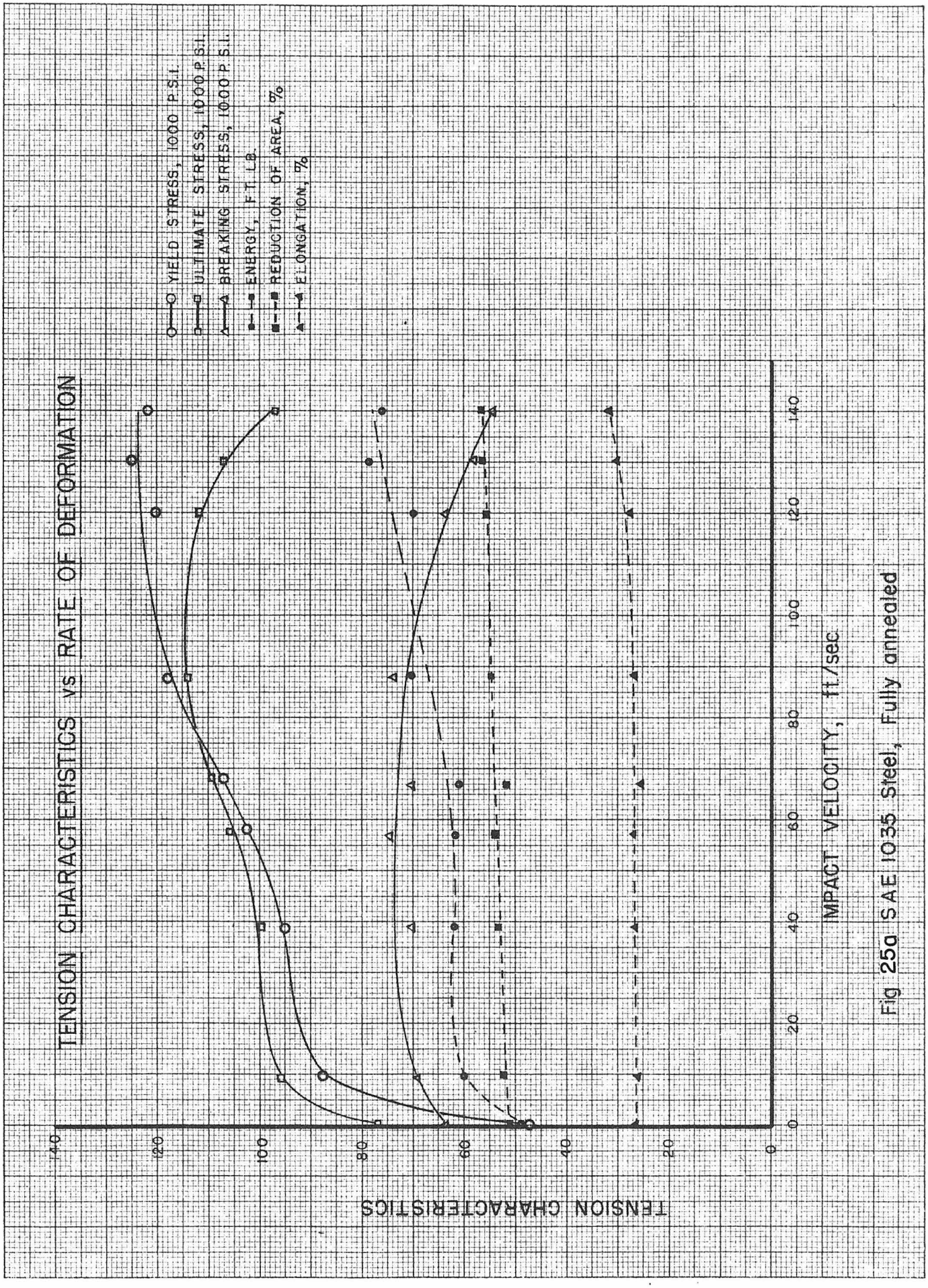


Fig 25a SAE 1035 Steel, Fully annealed

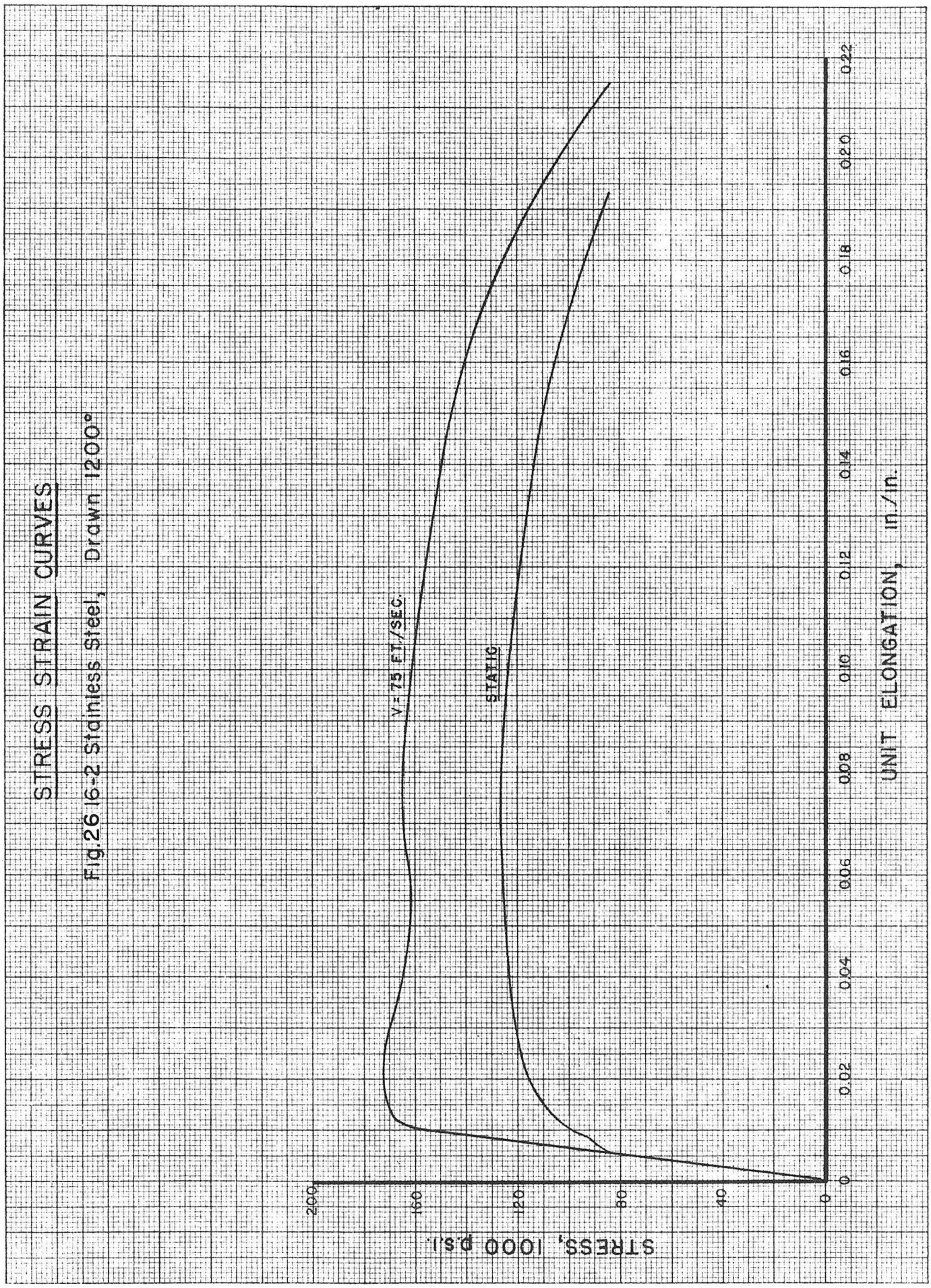
STRESS STRAIN CURVES
Fig. 26 16-2 Stainless Steel, Drawn 1200°
STRESS, 1000 p.s.i.
UNIT ELONGATION, in./in.
V= 75 FT./SEC.
STATIC
200
160
120
80
40
0
0
0.02
0.04
0.06
0.08
0.10
0.12
0.14
0.16
0.18
0.20
0.22

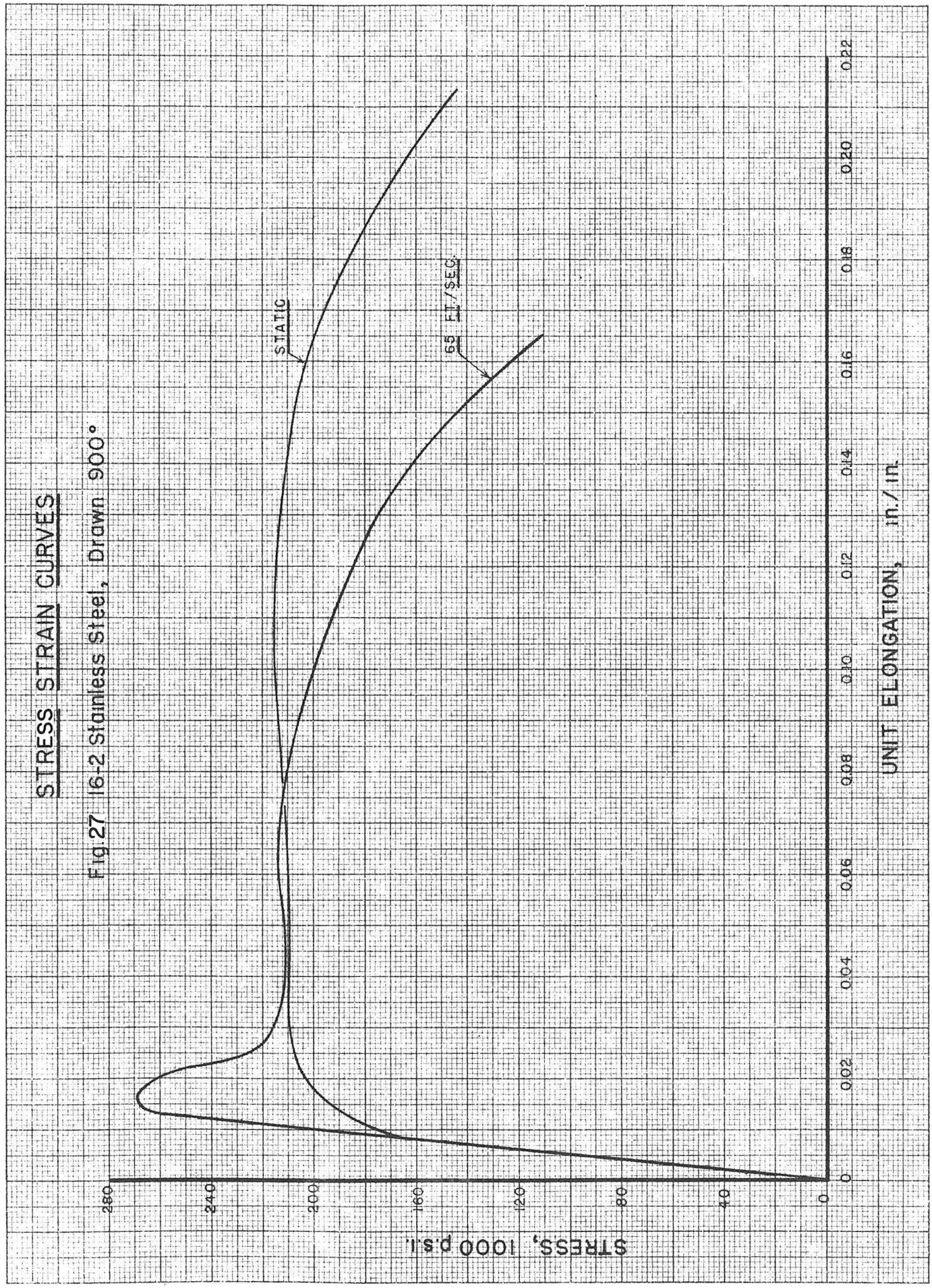
STRESS STRAIN CURVES
Fig 27 16-2 Stainless Steel, Drawn 900°
STATIC
65 FT/SEC
STRESS, 1000 p.s.i.
UNIT ELONGATION, in./in.
0
40
80
120
160
200
240
280
0.02
0.04
0.06
0.08
0.10
0.12
0.14
0.16
0.18
0.20
0.22

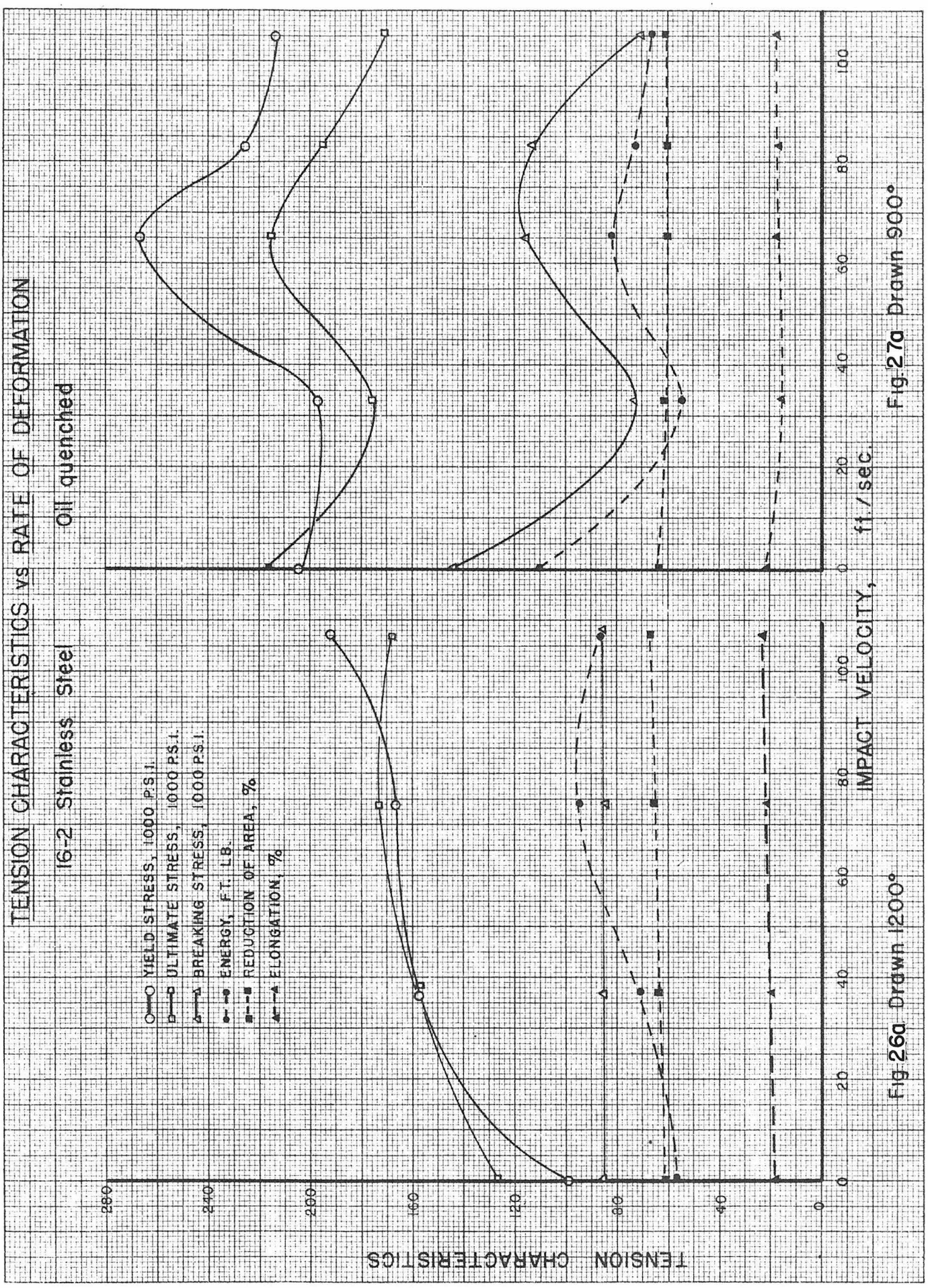


Fig 26a Drawn 1200°

Fig 27a Drawn 900°

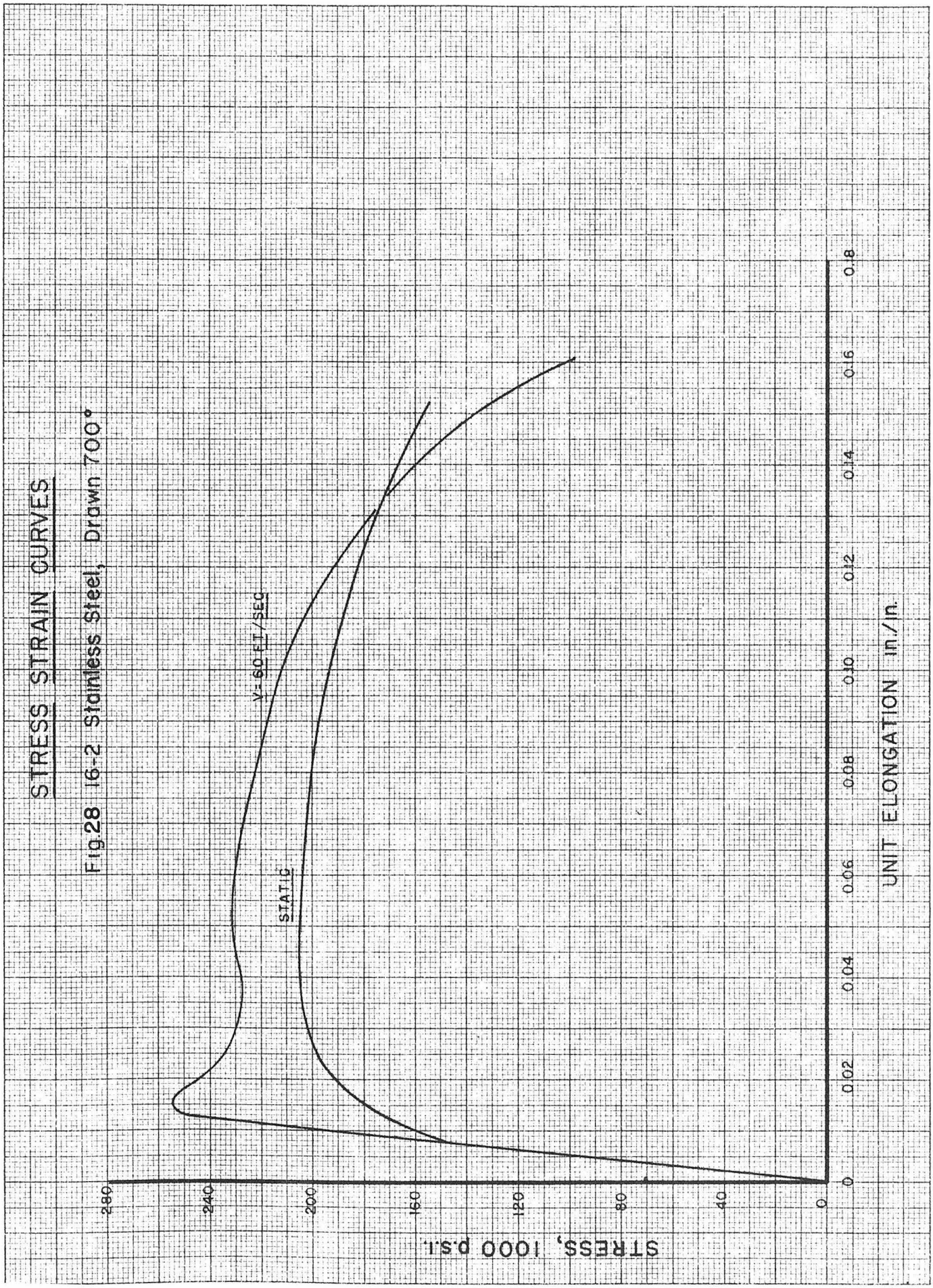
STRESS STRAIN CURVES
Fig.28 16-2 Stainless Steel, Drawn 700°
V= 60 FT/SEC
STATIC
STRESS, 1000 p.s.i.
UNIT ELONGATION in/in.
280
240
200
160
120
80
40
0
0
.002
.004
.006
.008
.010
.012
.014
.016
.018

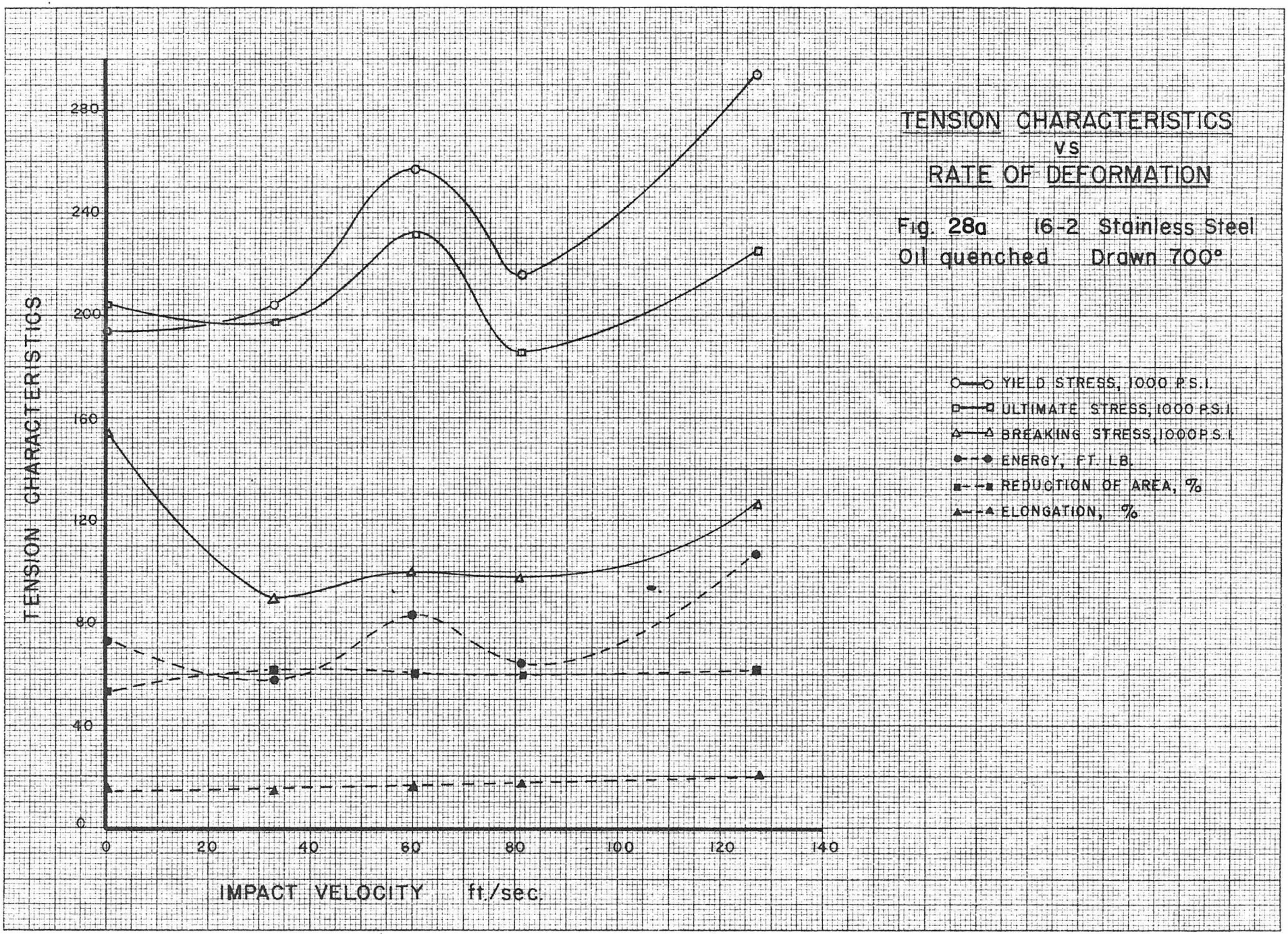
TENSION CHARACTERISTICS
VS
RATE OF DEFORMATION
Fig. 28a 16-2 Stainless Steel
Oil quenched Drawn 700°
YIELD STRESS, 1000 P.S.I.
ULTIMATE STRESS, 1000 P.S.I.
BREAKING STRESS, 1000 P.S.I.
ENERGY, FT. LB.
REDUCTION OF AREA, %
ELONGATION, %
TENSION CHARACTERISTICS
280
240
200
160
120
80
40
0
0
20
40
60
80
100
120
140
IMPACT VELOCITY ft./sec.

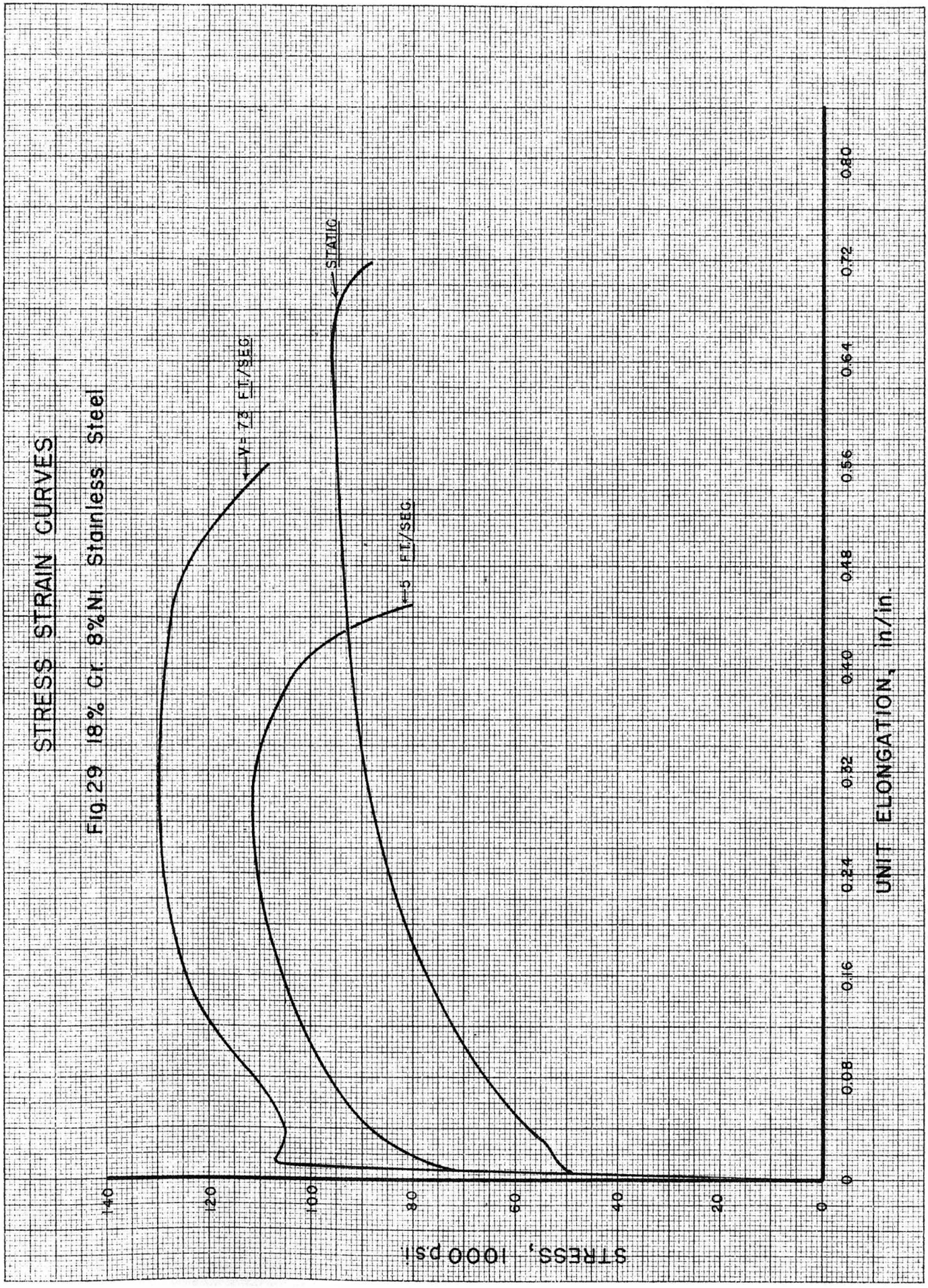
STRESS STRAIN CURVES
Fig. 29 18% Cr. 8% Ni Stainless Steel
STATIC
V= 73 FT./SEC
V=5 FT./SEC
STRESS, 1000 psi.
UNIT ELONGATION, in./in.
0
20
40
60
80
100
120
140
0.08
0.16
0.24
0.32
0.40
0.48
0.56
0.64
0.72
0.80

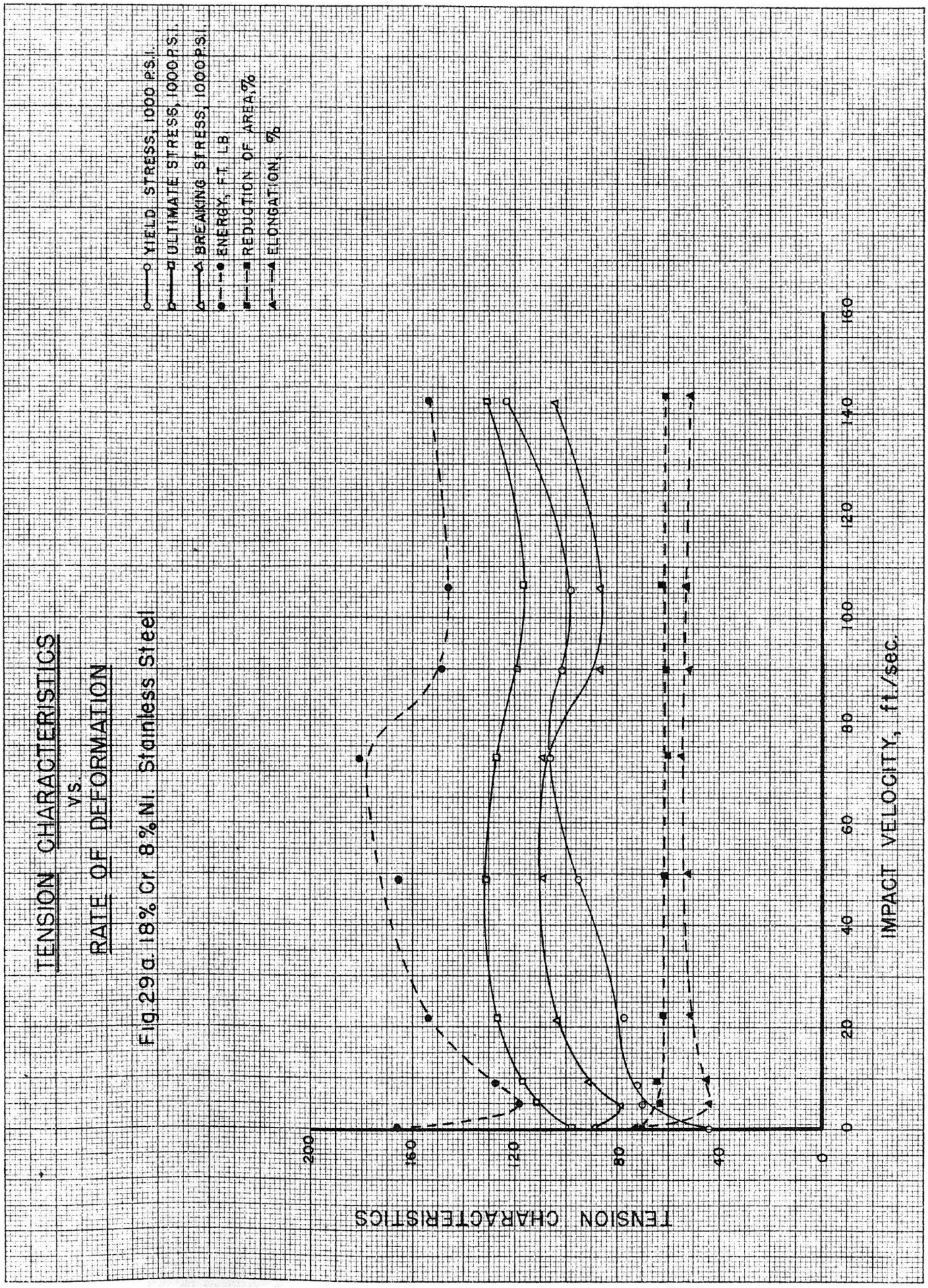
TENSION CHARACTERISTICS
vs.
RATE OF DEFORMATION
Fig. 29 a. 18% Cr. 8% Ni. Stainless Steel
YIELD STRESS, 1000 P.S.I.
ULTIMATE STRESS, 1000 P.S.I.
BREAKING STRESS, 1000 P.S.I.
ENERGY, F.T. LB
REDUCTION OF AREA, %
ELONGATION, %
TENSION CHARACTERISTICS
200
160
120
80
40
0
0
20
40
60
80
100
120
140
160
IMPACT VELOCITY, ft./sec.

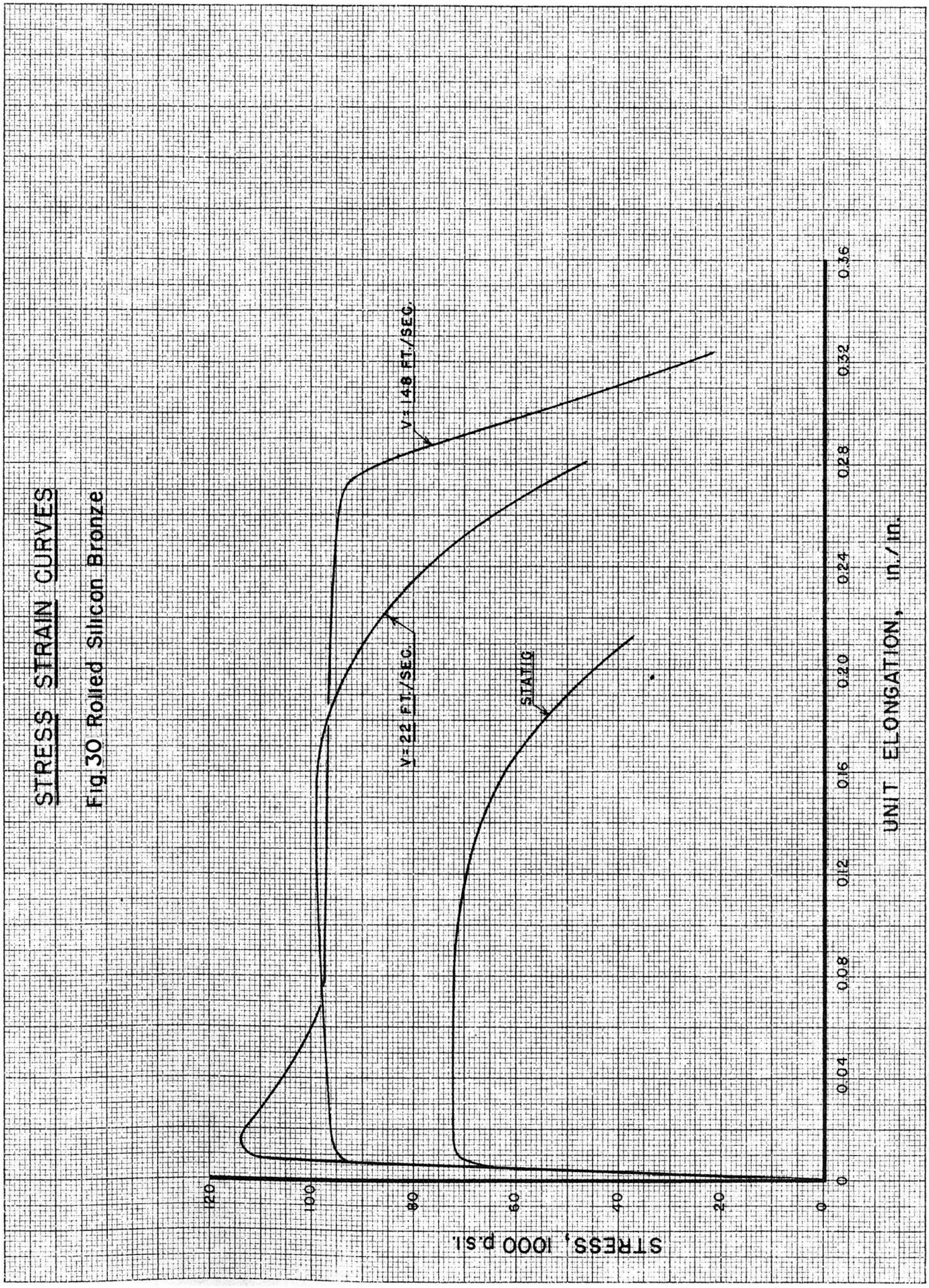
STRESS STRAIN CURVES
Fig.30 Rolled Silicon Bronze
V=148 FT./SEC.
V=22 FT./SEC.
STATIC
STRESS, 1000 p.s.i.
UNIT ELONGATION, in./in.
0
20
40
60
80
100
120
0.04
0.08
0.12
0.16
0.20
0.24
0.28
0.32
0.36

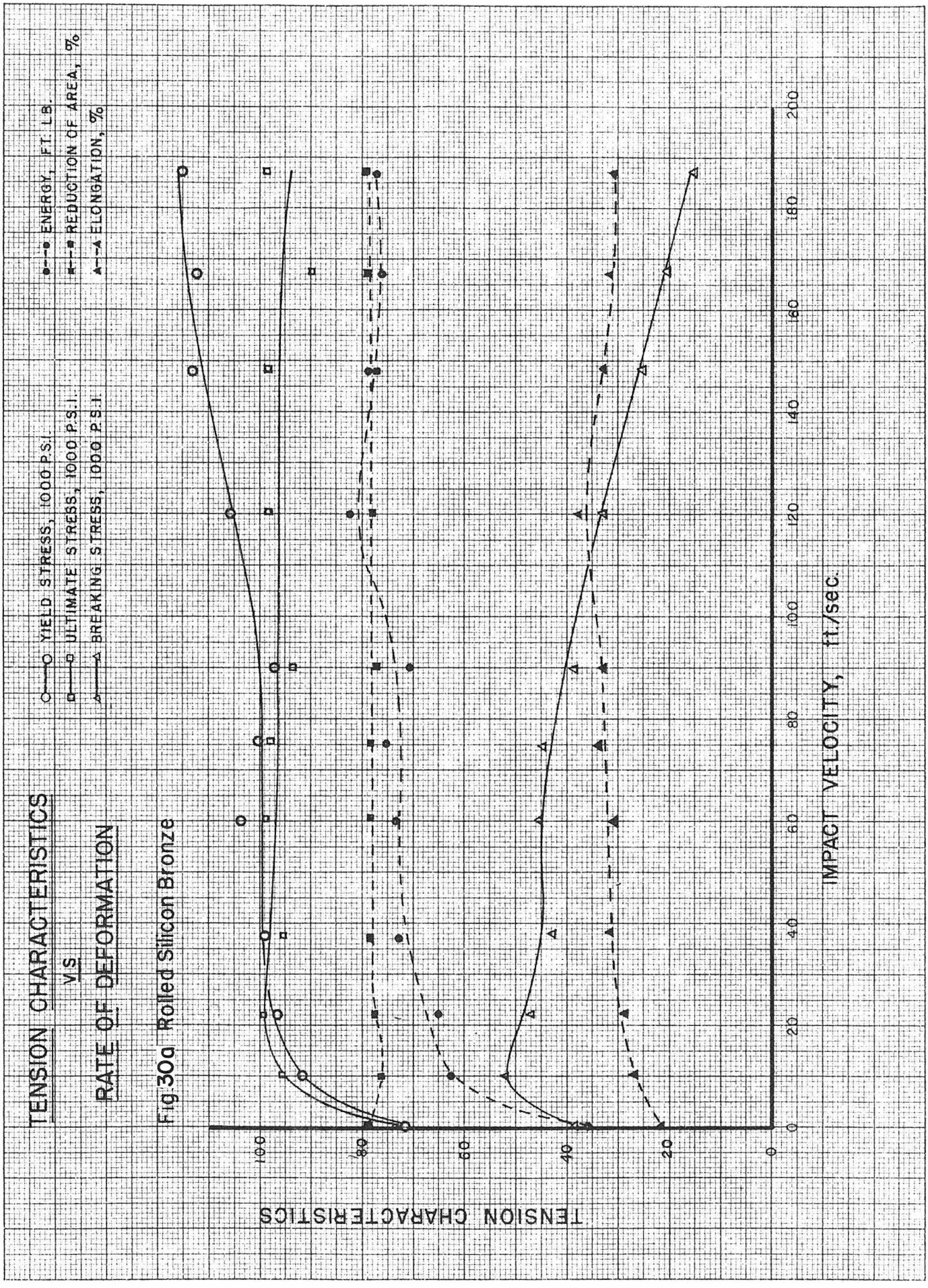


Fig. 30a Rolled Silicon Bronze

STRESS STRAIN CURVES

Fig. 31 17 S T Duralumin

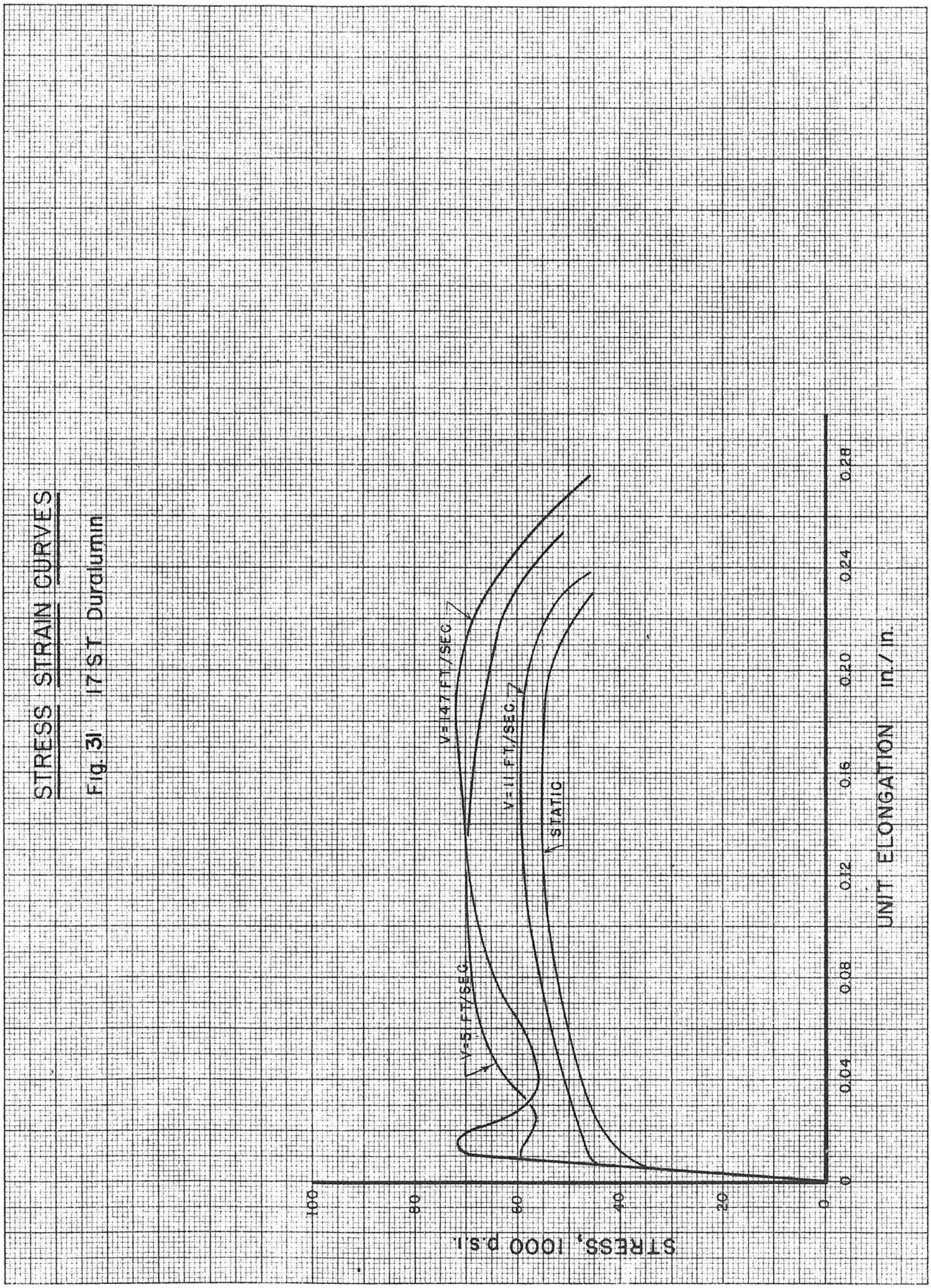

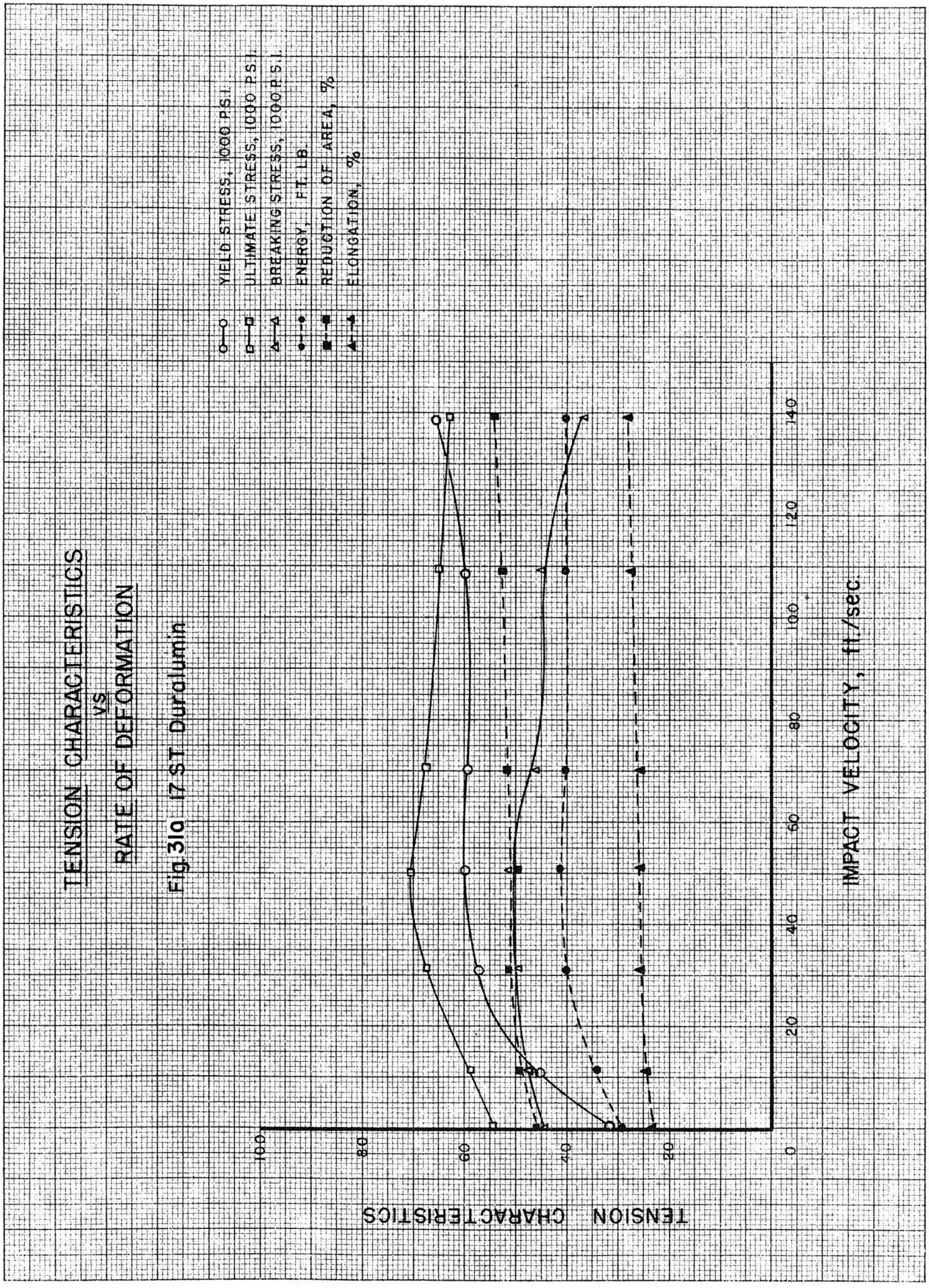


Fig. 31a 17 ST Duralumin

STRESS STRAIN CURVES

Fig. 32 24 S T Aluminum Alloy

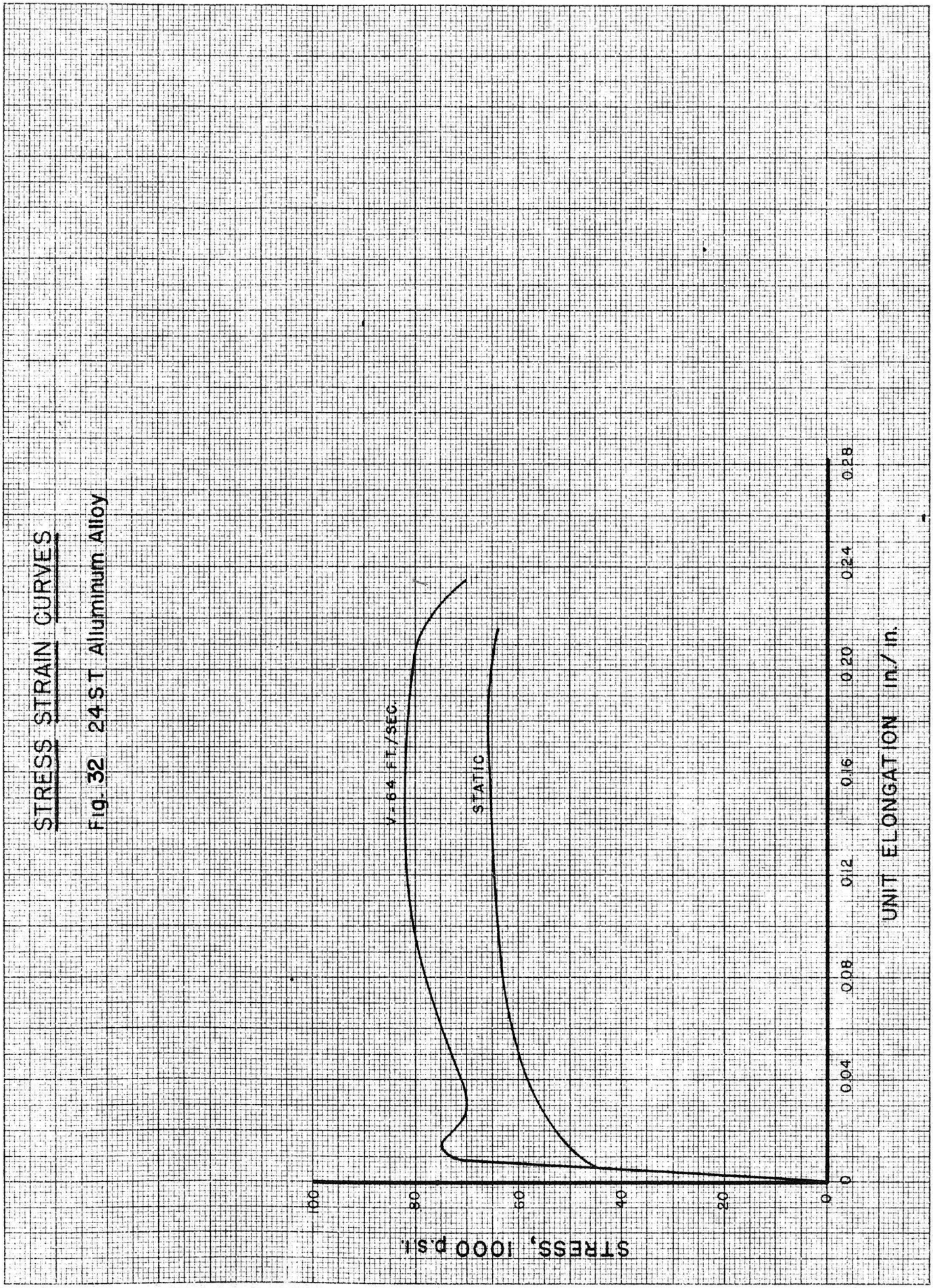

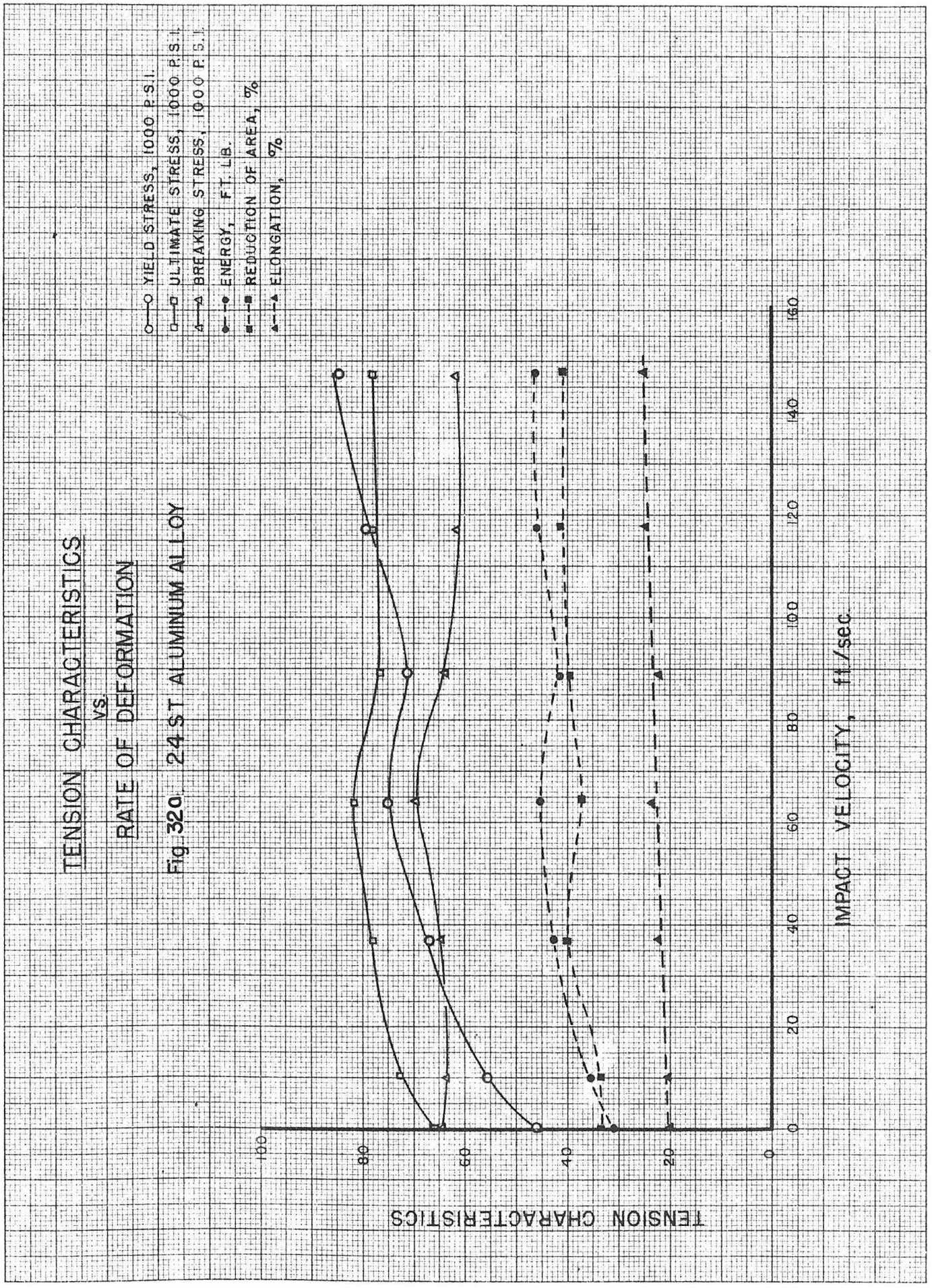
TENSION CHARACTERISTICS
vs.
RATE OF DEFORMATION
Fig 32a. 24ST ALUMINUM ALLOY
YIELD STRESS, 1000 P.S.I.
ULTIMATE STRESS, 1000 P.S.I.
BREAKING STRESS, 1000 P.S.I.
ENERGY, FT. LB.
REDUCTION OF AREA, %
ELONGATION, %
TENSION CHARACTERISTICS
100
80
60
40
20
0
0
20
40
60
80
100
120
140
160
IMPACT VELOCITY, ft./sec.

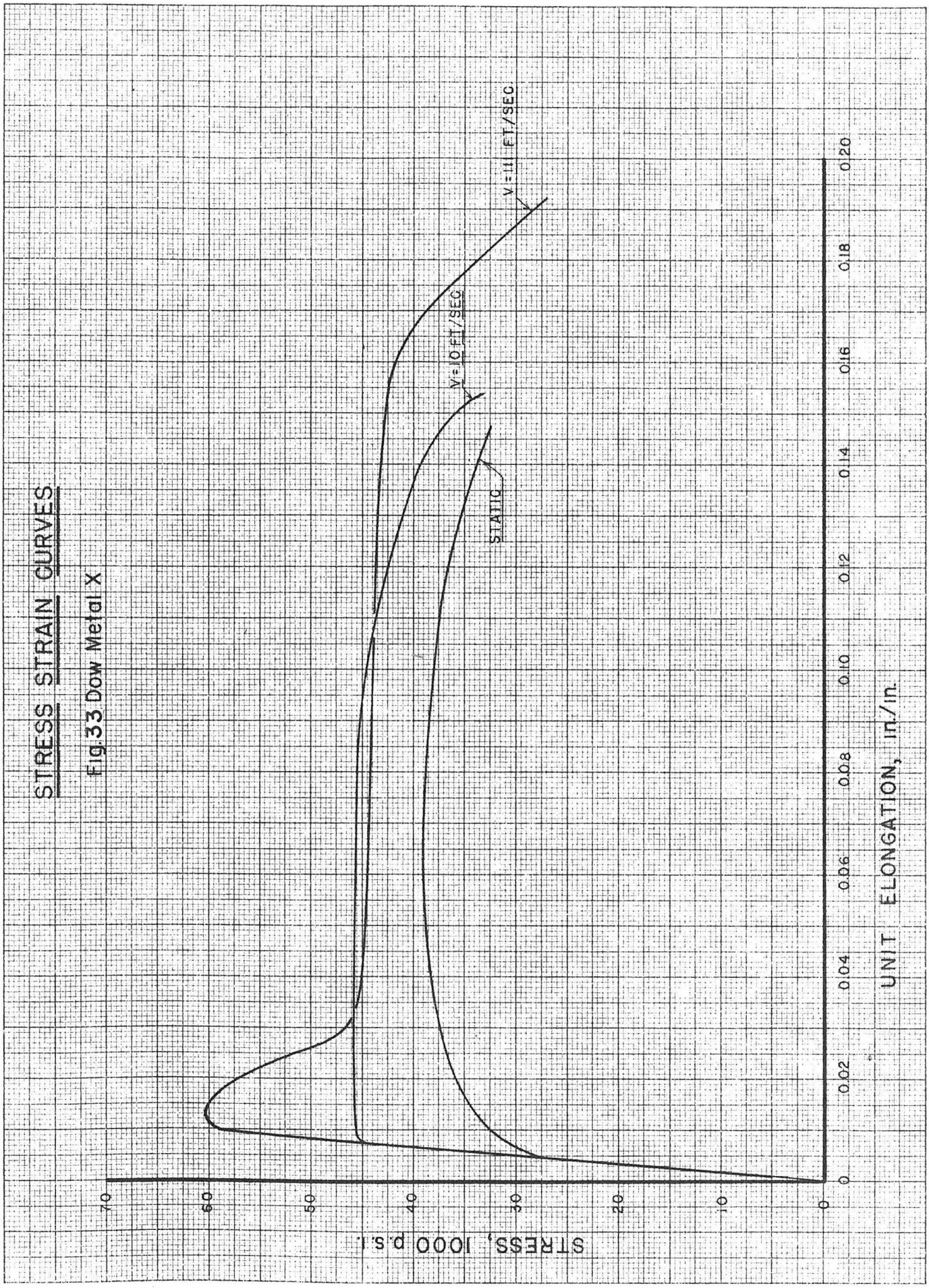
STRESS STRAIN CURVES
Fig.33 Dow Metal X
V=111 FT/SEC
V=10 FT/SEC
STATIC
STRESS, 1000 p.s.i.
UNIT ELONGATION, in./in.
0
10
20
30
40
50
60
70
0.02
0.04
0.06
0.08
0.10
0.12
0.14
0.16
0.18
0.20

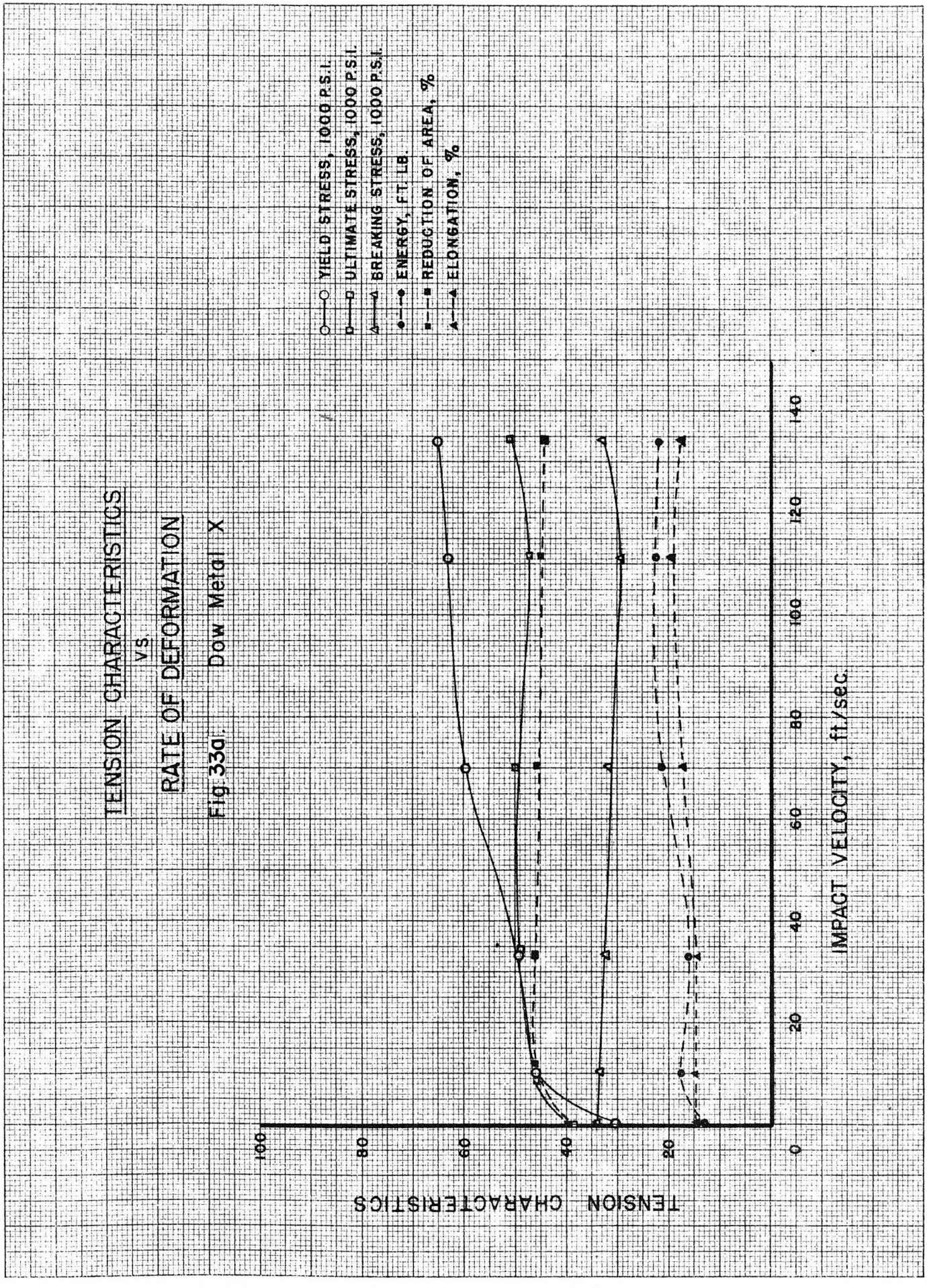
TENSION CHARACTERISTICS
vs.
RATE OF DEFORMATION
Fig. 33a. Dow Metal X
YIELD STRESS, 1000 P.S.I.
ULTIMATE STRESS, 1000 P.S.I.
BREAKING STRESS, 1000 P.S.I.
ENERGY, FT. LB.
REDUCTION OF AREA, %
ELONGATION, %
TENSION CHARACTERISTICS
100
80
60
40
20
0
0
20
40
60
80
100
120
140
IMPACT VELOCITY, ft./sec.

C. Discussion of Results.

As a result of the experimental work just outlined, it is possible to discuss the relative ability of engineering materials to withstand tension impact loading simulated by these testing conditions. From the results shown, it is seen that some materials show a marked increase in the dynamic properties over corresponding static values as the rate of deformation increases; while other materials are relatively unaffected.

The cold drawn S.A.E. 1112 steel indicates a marked rise in yield stress from 90,000 p.s.i. to 130,000 p.s.i. with an increase in rate of deformation from static to 20 feet per second; and the energy required to rupture the specimen rises from 26 to 47 foot-pounds in the same range. Above 20 feet per second the yield stress continues to rise, but the energy increases only slightly to 60 feet per second and then decreases, indicating that for the same elongations the plastic stresses are decreasing. The stress-strain diagrams of Figure 24 bear out these results.

Annealed S.A.E. 1035 steel shows a remarkable increase in yield stress from 47,000 p.s.i. to 92,000 p.s.i., an increase in ultimate stress from 75,000 p.s.i. to 100,000 p.s.i., and an energy rise from 49 foot-pounds to 62 foot-pounds with a change in rate of loading from static to 20 feet per second. At higher rates of deformation, the yield stress continues to rise to 125,000 p.s.i. at 140 feet per second, the ultimate stress rises to a maximum of 115,000 p.s.i. at 90 feet per second and then drops off gradually, while the energy continues to increase to 78 foot-pounds at 140 feet

per second. Reduction of area and per cent elongation show no abrupt changes over the entire velocity range.

With this and other materials, when the ultimate stress is reported smaller than the yield stress, there are indications of a marked decrease in the resistance to deformation beyond the yield strength, sometimes followed by a slight increase to the ultimate, as may be observed in Figure 25. This figure gives an excellent example of the increase in yield stress with a higher rate of deformation, preserving even at high speeds the same general form of the static stress-strain curve. As can be seen, the rise in yield strength is considerably greater than the rise in the ultimate. Other examples of this are shown in the stress-strain diagrams for 16% Cr - 2% Ni Stainless Steel, the Rolled Silicon Bronze, the 17ST Duralumin, and Dow Metal X. For an analysis of this marked rise in yield stresses, see page 74.

Specimens of 16% Cr - 2% Ni Stainless Steel, oil quenched from 1800° F., were tempered at three different temperatures, 1200° F., 900° F., and 700° F. Results of tests with this material may be compared in Figures 26a to 28a, at velocities up to 110 feet per second. Due to the few specimens available, these results are considered as preliminary; though they are quite interesting. Values of per cent elongation and reduction of area are almost identical for all three materials and remain constant over the velocity range; the stresses and absorbed energy, however, behave quite differently. For the weaker static material, tempered at 1200° F., moderate improvement

in properties is shown under rapid loading up to 80 feet per second, with the absorbed energy rising from 58 to 96 foot-pounds. The material tempered at 900° F. shows a decrease in ultimate and yield strength and energy up to 45 feet per second, but it is noted that the minimum values are not appreciably lower than the minimum values of the material tempered at 1200° F. The ultimate strength, yield strength and energy values of the material drawn at 700° F. do not change much up to speeds of 40 feet per second, after which the values increase appreciably. This might seem to indicate that the dynamic tensile properties of this steel are reasonably satisfactory in absolute value for any of these heat treatments. Lower Izod impact tests for the material tempered at 900° F. have indicated a notch sensitivity over other heat treatments, but its dynamic tensile properties are quite good, though not so high as for the specimens tempered at 700° F.

As shown in Figure 29a, the 18% Cr - 8% Ni Stainless Steel shows a very abrupt decrease from the static values of energy, elongation and breaking stress at low rates of deformation below ten feet per second. Above this speed, however, the energy values recover, apparently because the plastic stresses are continually increasing up to speeds around seventy feet per second. The yield stress rises above the static value abruptly with increased rate of loading, as shown in the stress-strain curves of Figure 29. The elongation and reduction of area drop rather abruptly from the static values of 70 per cent, and remain almost constant at 50 per cent and 60 per cent

respectively for all speeds above ten feet per second.

The remarkably large values of absorbed energy result from the great ductility of this material. Of all the materials tested, this 18% Cr - 8% Ni Steel absorbs the most energy up to fracture. The abrupt decrease in elongation cited above might be taken as an indication of a very low critical velocity of embrittlement inherent in the material itself. However, it seems more likely that this characteristic results from the combined effect of the time of deformation on the plastic yielding, and on the plastic stresses. Under static loading, this material does not come to equilibrium like other materials tested, but continues to deform plastically with time. With low speeds of impact, as at five feet per second, less time exists for this plastic deformation, hence the elongation is much less. At higher rates of loading, the elongation does not change appreciably, but the increasing stress values produce a rise in the energy absorbed. Consequently, this does not seem to be a "critical velocity" phenomenon, as previously suspected from the results of preliminary tests on this material and as discussed by D. S. Clark and G. Datwyler.[14]

Further detailed investigation with this stainless steel at much slower rates of loading (from one inch per second to five feet per second) would be of value in determining the properties of this particular material.

It is pertinent to call attention to Figures 20 to 23, presenting the ratio of dynamic to static values of yield stress,

absorbed energy, per cent elongation and reduction of area. These curves indicate the relative ability of the materials to withstand dynamic loads compared to static loads. For the ferrous group, and particularly for the 16% Cr - 2% Ni steels, the curve for the stainless steel tempered at 900° F. is below all others. It may be stated here that heat treatment is a factor to be investigated further in discussing the ability of a material to withstand shock stresses. Though this same stainless steel drawn at 900° F. is consistently weaker under dynamic conditions compared to its static behavior, the absolute physical values of the properties are high enough to classify it as a tough, strong steel, particularly for static service conditions.

In the case of the rolled Silicon Bronze, a large rise in yield and ultimate stresses and energy values occurs between the static tests and those at 25 feet per second, beyond which the values remain essentially constant up to the limit of speed investigated. This material shows clearly the development of a high yield stress followed by a decrease in resistance to plastic flow at higher velocities of loading. (See Figure 30.) Figures 21a and 22a indicate that the ratios of dynamic to static elongation and energy absorbed are superior to those of the other non-ferrous alloys tested. Of all the materials tested, this material alone indicates no variation in maximum reduction of area from 77 per cent for all velocities of loading. The breaking stress rises to a maximum at 10 feet per second, and then decreases gradually. In terms of the cohesive

strength for an amount of plastic deformation corresponding to 77 per cent reduction of area, this would indicate that the rate of deformation has the effect of increasing the cohesive stress for velocities up to 10 feet per second, but of lowering the cohesive strength at higher speeds.

In the cases of the light alloys, 17ST Duralumin, 24ST Aluminum alloy, and Dow Metal X, definite rises in yield stress and absorbed energy are again found with increased speeds of impact. All these show a slight general increase in the dynamic elongation and reduction of area. In the main, the 24ST alloy shows superior strength and higher values of energy absorbed compared to 17ST. These materials also exhibit a high dynamic yield in the form of a peak increasing in height with speed of loading.

It is significant to report that, for the range of velocities used, none of the materials shows a definite "critical velocity of embrittlement," or rate of deformation at which the energy required for rupture decreases sharply. Considerable precautions were taken to investigate two materials, notably rolled Silicon Bronze and annealed S.A.E. 1035 Steel, which have been reported by other investigators to show this phenomenon very definitely at specific rates of loading, i.e., 90 feet per second and 35 feet per second respectively. It is believed that such a characteristic can be conclusively proved or disproved only on the basis of stress-strain considerations, and not on energy considerations alone,[11] as had been done by others in the case of these materials. Present results do not demonstrate

this phenomenon.

It is also believed that such embrittlement, if it exists, must be accompanied by a marked and continual decrease in the per cent elongation and reduction of area. Examination of Figures 22 and 23 fails to disclose any evidence of such an occurrence at rates of loading here used. More recent preliminary tests on rolled Silicon Bronze at impact speeds of 250 feet per second have shown absolutely no change in the ductility from the values of elongation and reduction of area indicated at lower speeds.

Further investigation of this phenomenon should be made in connection with much higher speeds of loading, before this matter can be decided upon.

Inspection of Figures 20a and 21a shows several peaks and depressions in the dynamic energy and yield stresses of Dow Metal and Stainless Steel at certain velocities of loading. No conclusion has been reached as to their absolute accuracy or as to their cause. However, such changes in the characteristics of materials are often noted, due to temperature effects for example. Curves of ultimate stress, reduction of area, and per cent elongation show this familiar feature at different temperatures in the static tension test of a medium carbon steel[14]. It seems possible that such an occurrence as a function of velocity might be caused by a temperature effect occurring at the slip planes in the material during the instant of impact.

Reference was made on page 69 to the marked rise in the

dynamic stresses prior to plastic deformation, exhibited particularly in the stress-strain curves at high velocities for S.A.E. 1035 Steel, rolled Silicon Bronze, and 17ST Duralumin. An explanation of this rise in yield stress may be found on the basis of a force-wave analysis.

At higher rates of speed the entire fracture takes place during a surprisingly short time. Consider, for example, an initial speed of impact of 150 feet per second, and a total elongation of 0.25 inch in the one inch gage length of the specimen. The elastic deformation of the dynamometer during rupture amounts to perhaps 0.0005 inch; consequently the fixed end of the specimen may be considered essentially stationary during the test. The velocity of the disc is quite unchanged by the relatively small amount of energy required for fracture of the specimen. Therefore rupture must occur during the time required to move 0.25 inch at 150 feet per second: i.e., approximately 0.00014 second, or $\frac{1}{7200}$ second.

Lacking a basis for the contrary, it seems reasonable to assume that the modulus of elasticity of the specimen material is unchanged during rates of deformation as small as 150 feet per second, compared to the velocity of sound in the material. However, at such a rate of deformation, the material will behave during the elastic stage and prior to plastic flow very differently from a static tension test. Beginning at the instant of impact of the jaws on the tup, a stress-wave will pass from the tup down the specimen gage length, moving with the speed of sound in steel or about 203,000

inches per second. $V_s = \sqrt{Eg/w}$, where $E$ is the modulus of elasticity of steel and $w$ is the density of the material in pounds per cubic inch. The magnitude of this stress wave is computed as follows:

Assume $V_t$ is the tup velocity after impact, $V_s$ the stress-wave velocity, and $S$ the resulting stress intensity. In an interval of time dt, the wave will move $V_s \cdot dt$ inches along the specimen, and the resulting elongation of the specimen will be $\frac{S}{E} \cdot V_s dt$ inches. Ignoring plastic yield at first, this elongation will equal the forward motion of the tup, or $V_t \cdot dt$; consequently, $S = E \cdot \frac{V_t}{V_s}$. For a steel test specimen, and tup moving at 150 feet per second, the front of the wave of stress would have an intensity of $3 \cdot 10^7 \cdot \frac{150 \cdot 12}{203,000} \sim 270,000$ pounds per square inch.

This wave will travel down the one inch gage length in 1/203,000 second. From the far end of the specimen, where there is an abrupt change in section, a wave of the same velocity but of smaller intensity will travel down the dynamometer and a reflected wave of approximately equal intensity will travel back through the specimen, increasing the total stress intensity by a little less than 270,000 pounds per square inch at each reflection. If the intensity adds up so fast that the cohesive strength of the material is exceeded before plastic deformation occurs, a brittle break, without appreciable ductility, will occur. Usually, plastic yield will intervene unless extremely high impact rates are used; hence the necessary elongation can be furnished without calling for these very

high stresses. In other words, the stress wave will be damped out in two or three cycles. The crest of the wave may start out with the full computed height as given above, so that for an instant the material in the specimen is stressed above its normal elastic limit.

From a consideration of the cohesive strength theory expressed in Figures 1 and 2, it seems possible to define the critical velocity of embrittlement as that velocity of deformation above which the stress intensity in the tension wave exceeds the cohesive strength of the material. In this case, the high initial stress exceeds the resistance to fracture and produces a tensile break in the specimen before plasticity has an opportunity to relieve the situation. As a result, a brittle fracture might occur in an impact test on a material which statically shows considerable elongation and reduction of area.

From an energy viewpoint, this large rise in yield stresses, coupled with the possibility of a brittle fracture, may indicate that a specific material is unsafe under dynamic loading. There would be little assurance that the energy-absorbing capacity of the material would prevent outright failure under shock loads. If, however, the cohesive strength is not exceeded early in the deformation, this rise in the yield point may be considered an improvement in the elastic properties, giving an additional inherent factor of safety in design for dynamic service conditions. Therefore, added importance is attached to further investigation of this phenomenon of brittle

fracture, no specific example of which, however, has yet been found at velocities of impact reported in this thesis.

D. Limitations of This Investigation

It is to be emphasized that data represented in the curves of Figures 20 to 33 are not considered as exact and precise. In such testing equipment and with the complex technique described, including as it does a combination of mechanical, electrical, photographic, graphical and arithmetical procedures, there is of necessity a range of tolerances to be expected in the over-all accuracy of results. Again, such an investigation in a new field is not expected to establish quantitative laws on the basis of a few dozen or even a few hundred test specimens.

It can be stated with certainty, however, that digressive investigations concerning details of the equipment have been carried out as the apparatus was in process of development. These showed that the over-all range of quantitative results is accurate to plus or minus five per cent. This means that, whereas only two or three specimens of a given material have been broken at a given speed in this series of tests, a range of results of plus or minus five per cent is the maximum variation to expect from this equipment. In time, it is believed that the accuracy can be improved as simplifications of the apparatus are inaugurated.

For example, it is believed that an improved design of the force-measuring strain gage or dynamometer can be applied to the gage length of each specimen, thus improving the frequency characteristics

of the response of the recording unit. The natural frequency of the strain gage unit of Figure 12, used in the work reported above, is 35 kilocycles. For velocities of impact above 200 feet per second such a natural frequency is too low, since fracture can occur in a period of time corresponding to five or six cycles of the response. An improved strain gage winding can be obtained by winding a resistance pick-up directly to the shoulder of the specimen as shown in Figure 13. For such a dynamometer the frequency may be as high as 100 kilocycles. Difficulties of producing and calibrating such gages uniformly and in quantity have already been almost entirely eliminated.

Some trouble has been experienced at impact rates above 150 feet per second in preventing bending of the yokes, which are acted on by terrific inertia forces at the instant of impact with the jaws and tup. Improved design in this mechanism perhaps will permit simplification of its manufacture, permitting easier replacement.

The photographic technique might be simplified for recording great numbers of tests in a short time by installation of an automatic film changer or movie-camera in place of the contax film holder now used. It is to be noted that photographic enlargement of the test curves is made with the same lens and approximately the same size factor as used in taking the original photograph. Individual force calibrations on each test record are made to decrease further the source of error.

It is to be pointed out that even with supposedly identical specimens, tested in conventional manner in a static testing machine, with the period of fracture ideally lengthened to five or ten minutes, a range of results of three or four per cent may occur. Non-homogeneities in the material, machining effects (thermal and mechanical), as well as any accidental eccentricities in loading, all tend to produce variations in results.

Further idealization of the testing procedure would result from testing a large number, say 100, specimens of a given material at each rate of loading, and producing a probability curve for that particular speed. In such a manner, definite quantitative results could be assured.

## Chapter VI

## Summary and Conclusions

It has been the purpose of this thesis to present a suitable testing procedure for obtaining stress-strain diagrams for materials under tension impact loading. This is intended to offer a more logical impact test than preceding methods, in that it separates the effect of the speed of loading on the strength from other conflicting factors, and permits measuring more basic tensile characteristics than heretofore possible.

Tension properties of several different ferrous and non-ferrous alloys have been investigated at rates of loading from 10 to 200 feet per second, and the results are compared with corresponding values obtained from static tension tests.

Study of the resulting data shows conclusively that high velocity tests are essential to bring out the actual dynamic properties of materials. There is a very marked dynamic effect on the values of energy required to fracture specimens in tension. For no material investigated has the energy value failed to vary over the low velocity range, in direct contrast to the results of investigations made with pendulum equipment by other investigators. No critical velocity of embrittlement has been observed within the range of speeds used in this investigation, though such a phenomenon may occur at higher velocities of impact than used up to the present.

For many of the materials tested there is a relatively large rise in absorbed energy values and in yield stresses for rates of deformation up to 20 or 30 feet per second, after which the values tend to become more constant. Other materials, such as the 16% Cr - 2% Ni Stainless Steel drawn at 900° F., may show, however, a considerable weakness compared to the static properties when subjected to impact loads. This suggests that the effect of heat treatment may bear considerable investigation regarding tension impact properties before choosing materials for service conditions involving dynamic tension loading.

Up to loading speeds of 200 feet per second no appreciably abrupt variation in ductility is noted for these materials, except for the 18% Cr - 8% Ni Stainless Steel at speeds under 10 feet per second. Comparison of such tensile properties as absorbed energy, per cent elongation and reduction of area for various materials indicates that no single geometrical characteristic, such as change in length or area during fracture, can be used as an exact basis for comparing energy values or other strength characteristics under rapidly applied loads. Inspection of the stress-strain curves in Figure 24 checks this, for example, since stresses and elongations may vary independently.

The existence of abnormally high stresses in several materials during the instant before plastic flow has been shown at high rates of loading. An analytic explanation of this occurrence has been presented on the basis of a stress-wave analysis. Such a

calculation gives a reason for the possible occurrence of a brittle fracture at sufficiently high velocities of loading according to the cohesive strength theory, for materials normally ductile under static tension conditions. It is quite apparent that total energy values alone, determined by the conventional pendulum impact test for a single speed of impact, are not suitable criteria for serviceability under widely varying tension impact conditions.

There is evidence of a more complicated relation between the resistance to deformation and the cohesive strength of materials than has been suggested by the theory of Kuntze. The increasing elongation and reduction of area with higher velocities of impact do not seem to check this theory. It is possible that the cohesive strength may not be independent of the velocity of deformation. Tests on rolled Silicon Bronze at 77 per cent reduction of area give a contradictory effect of velocity on the cohesive strength of this material. Further investigation of this point may permit closer correlation of these test data with the true behavior of materials under dynamic conditions.

In conclusion, the development of stress-strain relations over an even wider range of speeds, and for many more metals and alloys, should present a useful basis for selecting materials for use in machine design and for structural parts subject to impact loading. It is hoped that increasing investigation of these tension impact properties as a function of heat treatment may prove of assistance both to the designer and to the metallurgist.

## REFERENCES


1. P. Ludwik, Elemente der Technologischen Mechanik, pp. 44, 47, Julius Springer, Berlin (1909).
2. Physikalische Zeitschrift, vol. 10, no. 12, p. 411 (1909).
3. L. Prandtl, "Ein Gedenkemodell zur kinetischen Theorie der festen Koerper," Zeitschrift fur angewandte Mathematik und Mechanik, p. 85 (1928).
4. Two symposiums on Impact Testing reported in Proceedings Am. Soc. Testing Materials; vol. 22, Part II, pp. 1-137 (1922), and vol. 38, Part II, pp. 21-157 (1938).
5. F. Koerber and H. Storp, "Uber den Kraftverlauf bei der Schlagpruefung," Mitteilungen des Kaiser Wilhelm Instituts fur Eisenforschung, Dusseldorf, vol. 7, pp. 81-97 (1925).
6. E. Honegger, "Schlagzerreissversuche an Aluminium und Kupfer," Bericht 95, Eidgehossische Materialprufungsanstalt an der E.T.H., Zurich, pp. 1-11, April 1935.
7. J. Weerts, "Dynamische und statische Zugversuche an Aluminium Einzelkrystalle," Dissertation, Berlin (1928).
8. Guillery, Engineering, January 12, 1906, p. 49.
9. H. F. Moore, "Measurement of the Force of Impact by Means of the Elastic Stretch of a Steel Bar," Proceedings Am. Soc. Testing Materials, vol. 22, Part II, p. 124 (1922).
10. D. W. Ginns, "The Mechanical Properties of Some Metals and Alloys Broken at Ultra-high Speeds," Journal Inst. Metals, vol. LXI, p. 61 (1937).

11. H. C. Mann, "High Velocity Impact Tests," Proceedings Am. Soc. Testing Materials, vol. 36, Part II, p. 85, (1936).

12. Impact Papers, Physico-Technical Institute, Leningrad, Journal of Technical Physics, USSR, vol. IX, no. 12 (1939). Translated by N. A. Ziegler, Crane Co. Research Laboratories.

13. W. Kuntze, "Questions of Technical Cohesion," Zeit. für Metallkunde, vol. 22, pp. 264-268 (1930).

14. D. S. Clark and G. Datwyler, "Stress-Strain Relations under Tension Impact Loading," Proceedings Am. Soc. for Testing Materials, vol. 38, Part II, p. 98 (1938).

15. S. Timoshenko and G. H. MacCullough, Elements of Strength of Materials, Second Edition, Van Nostrand, p. 314 (1940).

## ADDITIONAL BIBLIOGRAPHY

S. B. Russell, "Impact Testing Experiments," Transactions Am. Soc. of Civil Engineers, vol 39, p. 237 (1898).

A. A. Griffith, "Theory of Crack Strength vs. Atomic Strength," Phil. Trans., vol. 221, pp. 163-198 (1921).

O. V. Green and R. D. Stout, "Stress-Strain Characteristics of the Torsion Impact Test," Transactions Am. Soc. for Metals, vol. 28, p. 277 (1940).

M. Manjoine and A. Nadai, "High-Speed Tension Tests at Elevated Temperatures," Am. Soc. Testing Materials preprint no. 44, 1940.

M. Gensamer, "Static Crack Strength of Metals: Determination and Significance," Metal Progress, July 1940, p. 59.